5 El-Rayes BF, LoRusso PM. Targeting the epidermal growth factor receptor. *Br J Cancer* 2004; **91**: 418–24.
6 Sirotnak FM, Zakowski MF, Miller VA, Scher HI, Scher HI, Kris MG. Efficacy of cytotoxic agents against human tumor xenografts is markedly enhanced by coadministration of ZD1839 (Iressa), an inhibitor of EGFR tyrosine kinase. *Clin Cancer Res* 2000; **6**: 4885–92.
7 Herbst RS, Kies MS. ZD1839 (Iressa) in non-small cell lung cancer. *Oncologist* 2002; **7**: 9–15.
8 Okabe T, Okamoto I, Tamura K *et al.* Differential constitutive activation of the epidermal growth factor receptor in non-small cell lung cancer cells bearing EGFR gene mutation and amplification. *Cancer Res* 2007; **67**: 2046–53.
9 Asahina H, Yamazaki K, Kinoshita I. A phase II trial of gefitinib as first-line therapy for advanced non-small cell lung cancer with epidermal growth factor receptor mutations. *Br J Cancer* 2006; **95**: 998–1004.
10 Das AK, Sato M, Story MD *et al.* Non-small-cell lung cancers with kinase domain mutations in the epidermal growth factor receptor are sensitive to ionizing radiation. *Cancer Res* 2006; **66**: 9601–8.
11 Balak MN, Gong Y, Riely GJ *et al.* Novel D761Y and common secondary T790M mutations in epidermal growth factor receptor-mutant lung adenocarcinomas with acquired resistance to kinase inhibitors. *Clin Cancer Res* 2006; **12**: 6494–501.
12 Hay N, Sonenberg N. Upstream and downstream of mTOR. *Genes Dev* 2004; **18**: 1926–45.
13 Inoki K, Ouyang H, Li Y, Guan KL. Signaling by target of rapamycin proteins in cell growth control. *Microbiol Mol Biol Rev* 2005; **69**: 79–100.
14 Dobashi Y, Suzuki S, Matsubara H, Kimura M, Endo S, Ooi A. Critical and diverse involvement of Akt/mammalian target of rapamycin signaling in human lung carcinomas. *Cancer* 2009; **115**: 107–18.
15 Pal SK, Figlin RA, Reckamp KL. The role of targeting mammalian target of rapamycin in lung cancer. *Clin Lung Cancer* 2008; **9**: 340–5.
16 Campone M, Levy V, Bourbouloux E *et al.* Safety and pharmacokinetics of paclitaxel and the oral mTOR inhibitor everolimus in advanced solid tumours. *Br J Cancer* 2009; **100**: 315–21.
17 Wolpin BM, Hezel AF, Abrams T *et al.* Oral mTOR inhibitor everolimus in patients with gemcitabine-refractory metastatic pancreatic cancer. *J Clin Oncol* 2009; **27**: 193–8.
18 Chan S, Scheulen ME, Johnston S *et al.* Phase II study of Temsirolimus (CCI-779), a novel inhibitor of mTOR, in heavily pretreated patients with locally advanced or metastatic breast cancer. *J Clin Oncol* 2005; **23**: 5314–22.
19 Chang SM, Wen P, Cloughesy T *et al.* Phase II study of CCI-779 in patients with recurrent glioblastoma multiforme. *Invest New Drugs* 2005; **23** (4): 357–61.
20 Duran I, Kortmansky J, Singh D *et al.* A phase II clinical and pharmacodynamic study of Temsirolimus in advanced neuroendocrine carcinomas. *Br J Cancer* 2006; **95**: 1148–54.
21 Hess G, Herbrecht R, Romaguera J *et al.* Phase III study to evaluate temsirolimus compared with investigator's choice therapy for the treatment of relapsed or refractory mantle cell lymphoma. *J Clin Oncol* 2009; **27**: 3822–9.
22 Ohara T, Oto K, Miyoshi K *et al.* Sirolimus ameliorated post lung transplant chylothorax in lymphangioleiomyomatosis. *Ann Thorac Surg* 2008; **86**: e7–8.
23 Dudkin L, Dilling MB, Cheshire PJ *et al.* Biochemical correlates of mTOR inhibition by the rapamycin ester CCI-779 and tumor growth inhibition. *Clin Cancer Res* 2001; **7**: 1758–64.
24 deGraffenried LA, Friedrichs WE, Russell DH *et al.* Inhibition of mTOR activity restores tamoxifen response in breast cancer cells with aberrant Akt Activity. *Clin Cancer Res.* 2004;**10**: 8059–67.
25 Wan X, Shen N, Mendoza A, Khanna C, Helman LJ. CCI-779 inhibits rhabdomyosarcoma xenograft growth by an antiangiogenic mechanism linked to the targeting of mTOR/Hif-1a/VEGF signaling. *Neoplasia* 2006; **8**: 394–401.
26 Shirakawa Y, Naomoto Y, Kimura M *et al.* Topological analysis of p21WAF1/CIP1 expression in esophageal squamous dysplasia. *Clin Cancer Res* 2000; **6**: 541–50.
27 Berven LA, Crouch MF. Cellular function of p70S6K: a role in regulating cell motility. *Immunol Cell Biol* 2000; **78**: 447–51.
28 Hudes G, Carducci M, Tomczak P *et al.* Temsirolimus, interferon alfa, or both for advanced renal-cell carcinoma. *N Engl J Med* 2007; **356**: 2271–81.
29 Fang J, Ding M, Yang L, Liu LZ, Jiang BH. PI3K/PTEN/AKT signaling regulates prostate tumor angiogenesis. *Cell Signal* 2007; **19**: 2487–97.
30 Del Bufalo D, Ciuffreda L, Trisciuoglio D *et al.* Antiangiogenic potential of the mammalian target of rapamycin inhibitor temsirolimus. *Cancer Res* 2006; **66**: 5549–54.
31 Kallio PJ, Wilson WJ, O'Brien S, Makino Y, Poellinger L. Regulation of the Hypoxia-inducible Transcription Factor 1α by the Ubiquitin-Proteasome Pathway. *J Biol Chem* 1999; **274**: 6519–25.
32 Zhong H, De Marzo AM, Laughner E *et al.* Overexpression of hypoxia-inducible factor 1alpha in common human cancers and their metastases. *Cancer Res* 1999; **59**: 5830–5.
33 Sun SY, Rosenberg LM, Wang X *et al.* Activation of Akt and eIF4E survival pathways by rapamycin-mediated mammalian target of rapamycin inhibition. *Cancer Res* 2005; **65**: 7052–8.
34 Boffa DJ, Luan F, Thomas D *et al.* Rapamycin inhibits the growth and metastatic progression of non-small cell lung cancer. *Clin Cancer Res* 2004; **10**: 293–300.
35 Pullen N, Thomas G. The modular phosphorylation and activation of p70s6k. *FEBS Lett* 1997; **410**: 78–82.
36 Soria JC, Lee HY, Lee JI *et al.* Lack of PTEN expression in non-small cell lung cancer could be related to promoter methylation. *Clin Cancer Res* 2002; **8**: 1178–84.
37 Anagnostou VK, Bepler G, Syrigos KN *et al.* High expression of mammalian target of rapamycin is associated with better outcome for patients with early stage lung adenocarcinoma. *Clin Cancer Res* 2009; **15**: 4157–64.
38 Dancey J. mTOR signaling and drug development in cancer. *Nat Rev Clin Oncol* 2010;7:209–19.
39 Kodama Y, Baxter RC, Martin JL. Insulin-like growth factor-I inhibits cell growth in the a549 non-small lung cancer cell line. *Am J Respir Cell Mol Biol* 2002; **27**: 336–44.
40 Cohen A, Hall MN. An amino acid shuffle activates mTORC1. *Cell* 2009; **136**: 399–400.
41 Kleijn M, Proud CG. Glucose and amino acids modulate translation factor activation by growth factors in PC12 cells. *Biochem J* 2000; **347**: 399–406.

Supporting Information

Additional Supporting Information may be found in the online version of this article:

Fig. S1. Temsirolimus induces $p21^{cip1}$ expression in none-small-cell lung carcinoma cells.

Fig. S2. Proliferation and apoptosis in tumor tissues after temsirolimus treatment in mice.

Fig. S3. Inhibition of mTOR by temsirolimus decreases the expression of proangiogenic effectors.

Please note: Wiley-Blackwell are not responsible for the content or functionality of any supporting materials supplied by the authors. Any queries (other than missing material) should be directed to the corresponding author for the article.

REPORT

Cell Cycle 10:16, 2737-2741; August 15, 2011; © 2011 Landes Bioscience

Tumor-selective adenoviral-mediated GFP genetic labeling of human cancer in the live mouse reports future recurrence after resection

Hiroyuki Kishimoto,[1-3] Ryoichi Aki,[1,2] Yasuo Urata,[4] Michael Bouvet,[2] Masashi Momiyama,[1,2] Noriaki Tanaka,[3] Toshiyoshi Fujiwara[3] and Robert M. Hoffman[1,2,*]

[1]AntiCancer, Inc.; [2]Department of Surgery; University of California at San Diego; San Diego, CA USA; [3]Division of Surgical Oncology; Department of Surgery; Okayama University Graduate School of Medicine; Dentistry and Pharmaceutical Sciences; Okayama, Japan; [4]Oncolys BioPharma, Inc.; Tokyo, Japan

Key words: green fluorescent protein, adenovirus, cancer labeling, in situ, fluorescence-guided surgery, recurrence, detection

We have previously developed a telomerase-specific replicating adenovirus expressing GFP (OBP-401), which can selectively label tumors in vivo with GFP. Intraperitoneal (i.p.) injection of OBP-401 specifically labeled peritoneal tumors with GFP, enabling fluorescence visualization of the disseminated disease and real-time fluorescence surgical navigation. However, technical problems of removing all cancer cells still remain, even with fluorescence-guided surgery. In this study, we report that in vivo OBP-401 labeling of tumors with GFP before fluorescence-guided surgery reports cancer recurrence after surgery. Recurrent tumor nodules brightly expressed GFP, indicating that initial OBP-401-GFP labeling of peritoneal disease was genetically stable such that proliferating residual cancer cells still express GFP. In situ tumor labeling with a genetic reporter has important advantages over antibody and other non-genetic labeling of tumors, since residual disease remains labeled during recurrence and can be further resected under fluorescence guidance.

Introduction

Green fluorescent protein (GFP) serves as a very bright genetic reporter to detect metastatic cancer in mouse models.[1-3] Initially, cancer cells were transduced in vitro with GFP using various types of genetic vectors and then implanted in mouse models. Potential clinical application of GFP became possible when it was demonstrated that retroviruses containing GFP could label disseminated cancer in situ in mouse models.[4] Subsequently, selective in vivo GFP labeling of tumors was performed with OBP-401, a replicating adenovirus[5,6] that contains a replication cassette with the human telomerase reverse transcriptase (hTERT) promoter driving the expression of the viral *E1* genes, and the inserted *GFP* gene. Virus replication and hence *GFP* gene expression occur only in the presence of an active telomerase, i.e., in malignant tissue.[6] The OBP-401 virus was first tested by injection directly into HT-29 human colon tumors, orthotopically implanted into the rectum in BALB/c *nu/nu* mice. Subsequent para-aortic lymph node metastasis was observed by laparotomy under fluorescence.[6] We then developed a major enhancement of cancer surgical navigation in orthotopic mouse models of cancer, using in vivo selective fluorescent tumor labeling with OBP-401 GFP. Bright GFP fluorescence clearly illuminated the tumor boundaries and facilitated detection of the smallest disseminated disease lesions.[7]

Fluorescence-guided surgical navigation with tumors labeled in vivo with OAP-401 GFP was demonstrated in nude mouse models that represent difficult surgical challenges for the resection of widely disseminated cancer. HCT-116, a model of intraperitoneal disseminated human colon cancer, was labeled by virus injection into the peritoneal cavity. A549, a model of pleural dissemination of human lung cancer, was labeled by OBP-401 virus administered into the pleural cavity. Only the malignant tissue fluoresced brightly in both models. Further, we showed that OBP-401 could visualize liver metastases by tumor-specific expression of the GFP gene after portal venous or i.v. administration. Selective metastatic tumor labeling with GFP and killing by systemic administration of telomerase-dependent adenoviruses suggesting that liver metastasis is also a candidate for fluorescence-guided surgery.[8]

However, even fluorescence-guided surgery may still result in residual disease. The present report demonstrates proliferating residual disease remains stably labeled with OBP-401 GFP and is readily detected for further resection, suggesting that genetic-reporter labeling of tumors has advantages over non-genetic labeling of tumors for fluorescence-guided surgery.

Results and Discussion

Labeling peritoneal carcinomatosis with OBP-401-GFP. Peritoneal carcinomatosis was induced in the abdominal cavity of nude mice by i.p. implantation of HCT-116-RFP human colorectal cancer cells. Twelve days after implantation, 1 x 10^8 PFU

*Correspondence to: Robert M. Hoffman; Email: all@anticancer.com
Submitted: 06/01/11; Revised: 06/09/11; Accepted: 06/10/11
DOI: 10.4161/cc.10.16.16756

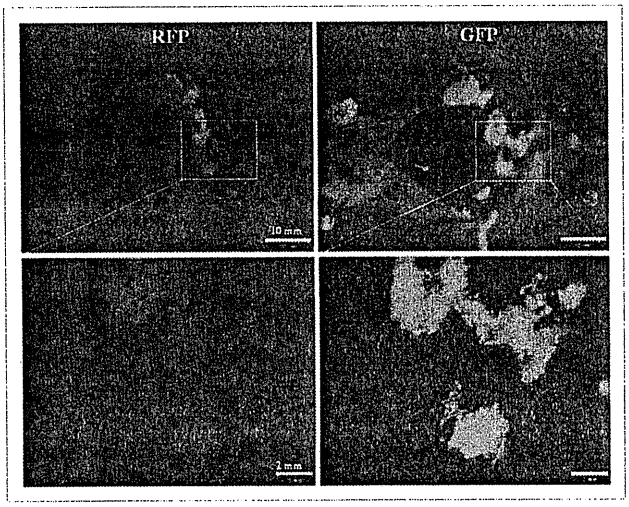

Figure 1. In situ genetic labeling of disseminated peritoneal carcinomatosis. Red fluorescence indicates HCT-116-RFP-expressing disseminated nodules (left). Peritoneal disseminated HCT116-RFP cells were labeled by GFP after i.p. injection of OBP-401 (right). Fluorescence imaging revealed co-localization of red and green fluorescence.

OBP-401 were injected intraperitoneally. Disseminated HCT-116-RFP nodules expressed GFP fluorescence induced by OBP-401 as well as the endogenous RFP fluorescence when imaged 5 d later (Fig. 1). RFP fluorescence was essentially coincident with that of GFP, indicating that i.p. injection of OBP-401 efficiently labeled disseminated tumors with GFP.

Stability of OBP-401-GFP expression in tumors. In order to determine stability of GFP expression in OBP-401 labeled tumors, HCT-116-RFP tumors were collected by peritoneal lavage from the abdominal cavity of mice 5 d after OBP-401 administration, put into culture in RPMI 1640 medium supplemented with 10% FBS and observed over time. Eight days after plating (13 d after viral administration), cancer cell colonies expressed both RFP and GFP (Fig. 2). The stability of GFP expression in OBP-401 labeled tumor cells suggests the potential of OBP-401 GFP labeling to detect recurrent tumors after attempted resection.

Fluorescence-guided resection of disseminated peritoneal tumors labeled with OBP-401 GFP. Five days after OBP-401 administration to mice with i.p. HCT-116, laparotomy was performed with the intent to remove all the intra-abdominal cancer using fluorescence-guided navigation under ketamine anesthesia (Fig. 3A and B). OBP-401 labeling and imaging made disseminated cancer nodules visible by GFP fluorescence, and complete resection was attempted (Fig. 3C–E). Tumors were efficiently resected, including those not visible under bright light, as we have previously reported in references 7 and 8.

In vivo detection of recurrent OBP-402-GFP labeled tumors after fluorescence-guided surgery. Tumors still recurred after attempted complete resection with fluorescence-guided surgery as visualized by GFP expression (Fig. 4). This result demonstrates that OBP-401 GFP labeling of peritoneal disseminated disease enables detection of tumor recurrence after fluorescence-guided surgery. Thus, OBP-401-GFP labeling is genetically stable and therefore proliferating residual disease continues to express GFP.

Tsien's laboratory has developed a method to label and visualize tumors during surgery using activatable cell-penetrating peptides (ACPPs), in which the fluorescently-labeled, polycationic cell-penetrating peptide (CPP) is coupled via a cleavable linker to a neutralizing peptide. Upon exposure to proteases expressed by tumors, the linker is cleaved, dissociating the inhibitory peptide and allowing the CPP to bind to and enter tumor cells. Animals whose tumors were resected with ACPPD guidance had better long-term tumor-free survival and overall survival than animals whose tumors were resected with traditional brightfield illumination only.[9]

Another approach to tumor labeling and fluorescence-guided surgery is with the use of labeled tumor-specific antibodies. A monoclonal antibody specific for CA19-9 was conjugated to a green fluorophore and delivered to tumor-bearing mice as a single intravenous (IV) dose. Intravital fluorescence imaging was used to localize metastatic pancreatic cancer in orthotopic mouse models 24 h after antibody administration. Using fluorescence imaging, the primary tumor was clearly visible at laparotomy, as were small metastases in the liver and spleen and on the peritoneum. The metastatic tumors, which were nearly impossible to see using standard brightfield imaging, demonstrated clear fluorescence under LED light excitation.[10]

We have also previously investigated the use of fluorophore-labeled anti-carcinoembryonic antigen (CEA) monoclonal antibody to aid in cancer visualization in nude mouse models of human colorectal and pancreatic cancer. Anti-CEA was conjugated with a green fluorophore. Subcutaneous, orthotopic primary and metastatic human pancreatic and colorectal tumors were easily visualized with fluorescence imaging after administration of conjugated anti-CEA. The fluorescence signal was detectable 30 min after systemic antibody delivery and remained present for 2 weeks, with minimal in vivo photobleaching after exposure to standard operating room lighting. Fluorescent anti-CEA administration improved ability to resect the labeled tumors under fluorescence guidance.[11]

Neither the ACPP nor labeled monoclonal antibodies, described above, involves genetic labeling of cancer cells, and thus recurrence would therefore not be detectable. In the present study, we selectively and efficiently labeled tumors with a genetic reporter, GFP, using a telomerase dependent adenovirus OBP-401. We demonstrated that tumors recurred after fluorescence-guided surgery and maintained GFP expression. Therefore, the detection of recurrence and future metastasis is possible with OBP-401 GFP labeling, since recurrent cancer cells stably express GFP, which is not possible with non-genetic labeling of tumors.

In clinical studies performed with OBP-401, circulating tumor cells (CTC) obtained from cancer patients were labeled with OBP-401 GFP ex vivo. OBP-401-GFP labeling greatly increased the detection of CTC.[12] Other targets for in vivo GFP labeling could include, for example, breast cancer emboli.[13] Specific labeling by GFP of cancer stem cells is also a promising approach.[14]

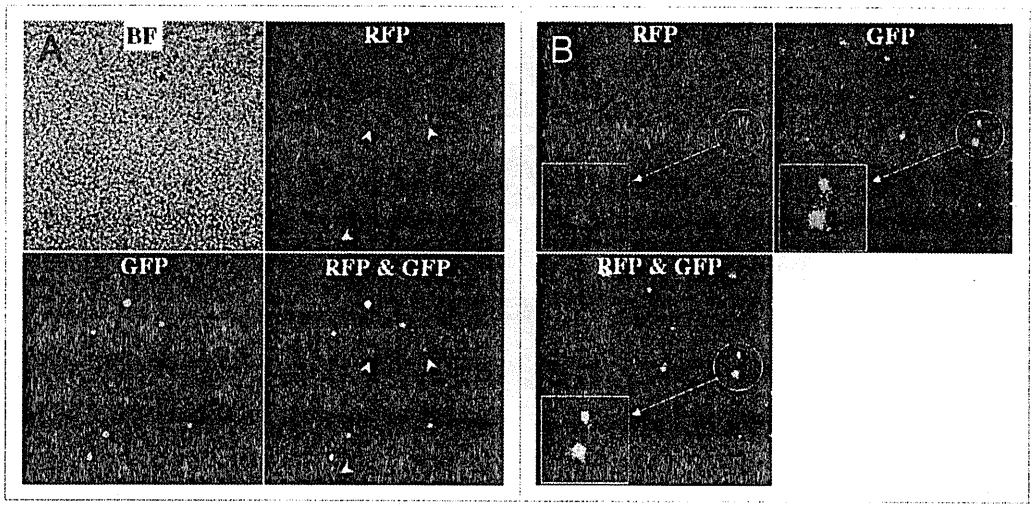

Figure 2. Genetic labeling of microscopic tumors. Cells collected by peritoneal lavage from the abdominal cavity of mice 5 d after OBP-401 treatment were plated and cultured with RPMI 1640 medium supplemented with 10% FBS. (A) Plating cells in the peritoneal lavage fluid (5 d after viral administration). Most RFP-expressing cancer cells expressed GFP fluorescence induced by OBP-401 as well, x200 magnification. White arrows: cells unlabeled with GFP. (B) 8 d after plating (i.e., 13 d after viral administration). Cancer cell colonies expressing RFP were observed in the culture dish under fluorescence microscopy. The cancer cells also expressed GFP induced by OBP-401. x40 magnification. Boxes highlight colonies indicated by white circles. Original magnification x100.

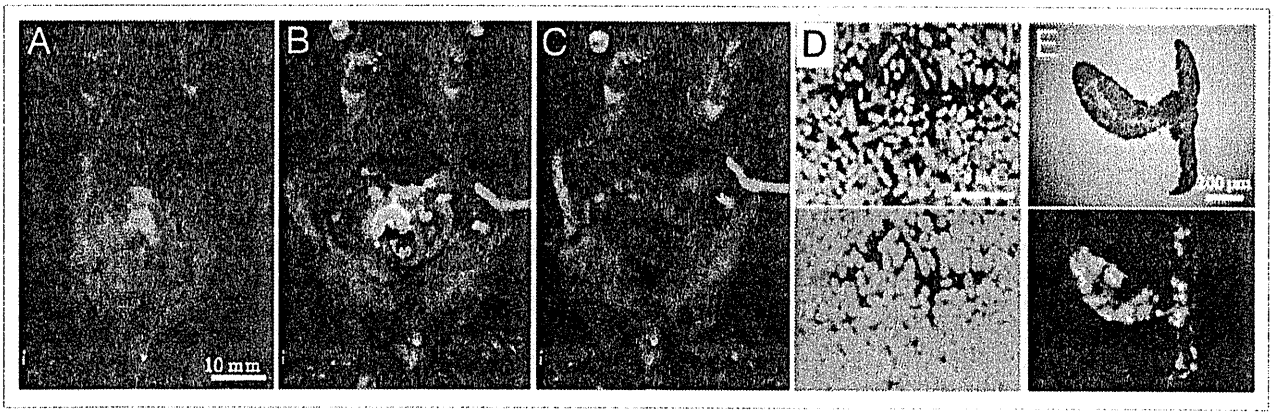

Figure 3. Fluorescence-guided resection of tumors labeled with GFP in situ. (A) Peritoneal disseminated nodules were labeled by GFP expression 5 d after OBP-401 virus administration. (B) Laparotomy was performed. (C) Disseminated nodules labeled with GFP were removed under GFP-guided surgical navigation. (D) Disseminated nodules removed under GFP-guided navigation. Top, bright field observation; bottom, fluorescent detection. (E) Section of disseminated nodules. Top, H&E section; bottom, frozen section with fluorescence detection.

Labeling of cancer stem cells is especially important, since at least some stem cells can now be imaged non-invasively.[15] The present report suggests the clinical potential of OBP-401 GFP labeling to improve the surgical outcome of cancer.

Materials and Methods

Recombinant adenovirus. Telomerase-specific replication-selective adenovirus OBP-401, containing the *GFP* gene under the control of the CMV promoter with the hTERT promoter driving the *E1A* and *E1B* genes, was constructed and produced as previously described in references 5 and 6.

Cell culture. The human colorectal cancer cell line HCT-116 was cultured in RPMI 1640 medium supplemented with 10% FBS.

Production of red fluorescent protein (RFP) retroviral vector. For RFP retrovirus production, the *Hind*III/*Not*I fragment from pDsRed2 (Clontech), containing the full-length RFP cDNA, was inserted into the *Hind*III/*Not*I site of pLNCX2 (Clontech) containing the neomycin-resistance gene. PT67, an NIH3T3-derived packaging cell line (Clontech) expressing the viral envelope, was cultured in DMEM supplemented with 10% FBS. For vector production, PT67 packaging cells, at 70% confluence, were incubated with a precipitated mixture of LipofectAMINE reagent

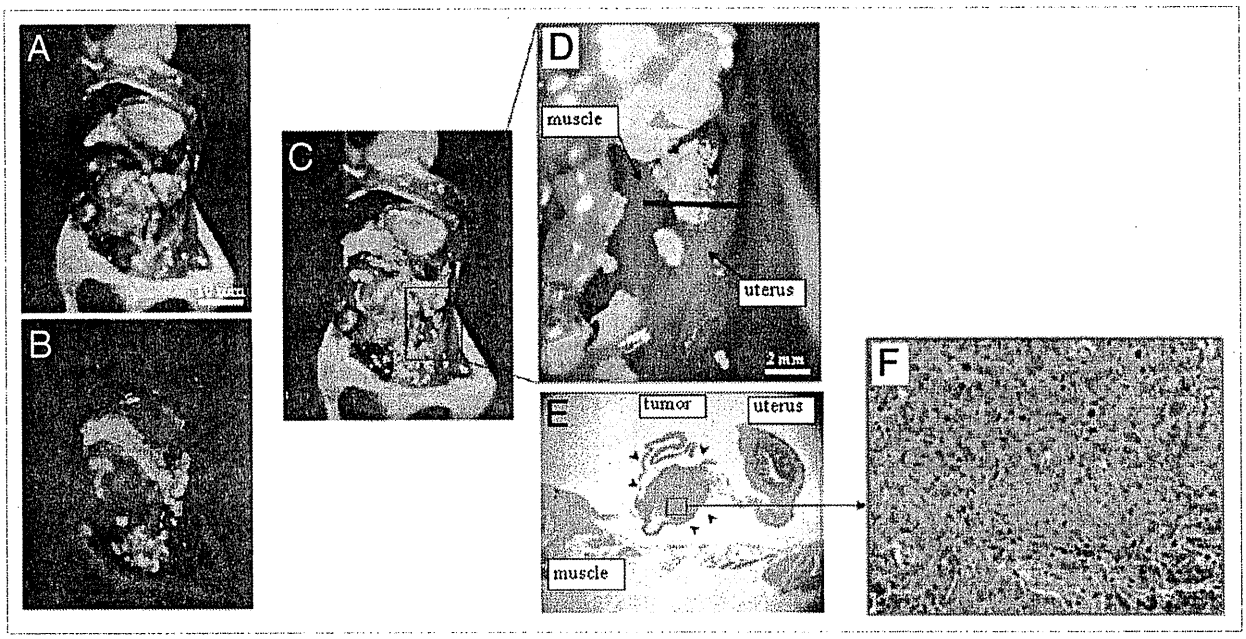

Figure 4. In vivo detection of recurrent tumors after fluorescence-guided surgery. (A) Brightfield observation several weeks after fluorescence-guided surgery of OBP-401 GFP-labeled tumors. Disseminated disease re-emerged. (B) Fluorescence observation of field observed by brightfield in (A). (C) Merge of (A and B). The red box outlines a region of (D) below. (D) Detail of the boxed region of (C). Black line indicates the direction of cross-sections. (E) Histologic sections stained with H&E showing that GFP-labeled lesions are recurrent tumor tissues (arrow heads). x40 magnification. (F) Detail of the boxed region of (E). x200 magnification.

(Life Technologies) and saturating amounts of pLNCX2-DsRed2 plasmid for 18 h. Fresh medium was replenished at this time. The cells were examined by fluorescence microscopy 48 h post-transduction. For selection of a clone producing high amounts of RFP retroviral vector (PT67-DsRed2), the cells were cultured in the presence of 200 to 1,000 μg/ml G418 (Life Technologies) for 7 d. The isolated packaging cell clone was termed PT67-DSRed2.[16]

RFP gene transduction of cancer cells. For RFP gene transduction, cancer cells were incubated with a 1:1 precipitated mixture of retroviral supernatants of PT67 cells and RPMI 1640 containing 10% FBS for 72 h. Fresh medium was replenished at this time. Tumor cells were harvested with trypsin/EDTA 72 h post-transduction and subcultured at a ratio of 1:15 into selective medium, which contained 200 μg/ml G418. To select brightly fluorescent cells, the level of G418 was increased up to 800 μg/ml in a stepwise manner. RFP-expressing cancer cells were isolated with cloning cylinders using trypsin/EDTA and were amplified by conventional culture methods in the absence of selective agent.[16]

Mice. Athymic nude mice were kept in a barrier facility under HEPA filtration and fed with autoclaved laboratory rodent diet. All animal studies were conducted in accordance with the principals and procedures outlined in the National Institute of Health Guide for the Care and Use of Laboratory Animals under Assurance Number A3873-1. All animal procedures were performed under anesthesia using s.c. administration of a ketamine mixture (10 μl ketamine HCL, 7.6 μl xylazine, 2.4 μl acepromazine maleate and 10 μl PBS).

In vivo fluorescence imaging. An Olympus OV100 Small Animal Imaging System (Olympus Corp., Tokyo, Japan) with macro and micro optics was used.[17] High-resolution images directly captured on a PC were processed and analyzed with the use of Adobe Photoshop Elements 4.0 software (Adobe).

Peritoneal carcinomatosis model with HCT-116 human colon cancer cells implanted in nude mice. Nude mice were intraperitoneally (i.p.) injected either with HCT-116 or HCT-116-RFP human colon cancer cells at a density of 3 x 10^6 in 200 μl PBS. Twelve days after tumor cell inoculation, mice were injected i.p. with OBP-401 at a dose of 1 x 10^8 PFU in 200 μl PBS. Five days after virus injection, the abdominal cavity was examined by fluorescence imaging, and mice were operated on with fluorescence guidance with the intent to resect all intra-abdominal tumor nodules under ketamine-induced anesthesia.

Collection of microscopic tumors from peritoneal lavage fluid of OBP-401 treated mice. Twelve days after nude mice were i.p. injected with HCT-116-RFP, 1 x 10^8 PFU OBP-401 were injected intraperitoneally. Five days after virus injection, mice were instilled with 8 ml PBS intraperitoneally. The abdomen was gently massaged and the peritoneal fluid was carefully aspirated using a 22-gauge needle. Approximately 6 ml peritoneal lavage fluid (PLF) were obtained from most mice. After filtering the PLF with a 40 μm cell strainer (BD, Franklin Lakes, NJ) in order to collect only microscopic tumors and/or cancer cells in the abdominal cavity, 3 ml of PLF were cultured on 6-well tissue culture plates. After incubation for 1 h, supernatants were carefully aspirated and 3 ml RPMI 1640 medium, containing 10% FBS,

were added to each well. The cells were further incubated at 37°C in a humidified atmosphere of 5% CO_2 and observed under fluorescence microscopy at day 0 and day 8 after collection of PLF.

Acknowledgments

This study was supported in part by National Cancer Institute grant CA132971 and CA142669.

References

1. Chishima T, Miyagi Y, Wang X, Yamaoka H, Shimada H, Moossa AR, et al. Cancer invasion and micrometastasis visualized in live tissue by green fluorescent protein expression. Cancer Res 1997; 57:2042-7; PMID: 9158003.
2. Yang M, Baranov E, Jiang P, Sun FX, Li XM, Li L, et al. Whole-body optical imaging of green fluorescent protein-expressing tumors and metastases. Proc Natl Acad Sci USA 2000; 97:1206-11; PMID: 10655509; DOI: 10.1073/pnas.97.3.1206.
3. Hoffman RM. The multiple uses of fluorescent proteins to visualize cancer in vivo. Nat Rev Cancer 2005; 5:796-806; PMID: 16195751; DOI: 10.1038/nrc1717.
4. Hasegawa S, Yang M, Chishima T, Miyagi Y, Shimada H, Moossa AR, et al. In vivo tumor delivery of the green fluorescent protein gene to report future occurrence of metastasis. Cancer Gene Ther 2000; 7:1336-40; PMID: 11059691; DOI: 10.1038/sj.cgt.0237.
5. Fujiwara T, Kagawa S, Kishimoto H, Endo Y, Hioki M, Ikeda Y, et al. Enhanced antitumor efficacy of telomerase-selective oncolytic adenoviral agent OBP-401 with docetaxel: preclinical evaluation of chemovirotherapy. Int J Cancer 2006; 119:432-40; PMID: 16477640; DOI: 10.1002/ijc.21846.
6. Kishimoto H, Kojima T, Watanabe Y, Kagawa S, Fujiwara T, Uno F, et al. In vivo imaging of lymph node metastasis with telomerase-specific replication-selective adenovirus. Nat Med 2006; 12:1213-9; PMID: 17013385; DOI: 10.1038/nm1404.
7. Kishimoto H, Zhao M, Hayashi K, Urata Y, Tanaka N, Fujiwara T, et al. In vivo internal tumor illumination by telomerase-dependent adenoviral GFP for precise surgical navigation. Proc Natl Acad Sci USA 2009; 106:14514-7; PMID: 19706537; DOI: 10.1073/pnas.0906388106.
8. Kishimoto H, Urata Y, Tanaka N, Fujiwara T, Hoffman RM. Selective metastatic tumor labeling with green fluorescent protein and killing by systemic administration of telomerase-dependent adenoviruses. Mol Cancer Ther 2009; 8:3001-8; PMID: 19887549; DOI: 10.1158/1535-7163.MCT-09-0556.
9. Nguyen QT, Olson ES, Aquilera TA, Jiang T, Scadeng M, Ellies LG, et al. Surgery with molecular fluorescence imaging using activatable cell-penetrating peptides decreases residual cancer and improves survival. Proc Natl Acad Sci USA 2010; 107:4317-22; PMID: 20160097; DOI: 10.1073/pnas.0910261107.
10. McElroy M, Kaushal S, Luiken G, Talamini MA, Moossa AR, Hoffman RM, et al. Imaging of primary and metastatic pancreatic cancer using a fluorophore-conjugated anti-CA19-9 antibody for surgical navigation. World J Surg 2008; 32:1057-66; PMID: 18264829; DOI: 10.1007/s00268-007-9452-1.
11. Kaushal S, McElroy MK, Luiken GA, Talamini MA, Moossa AR, Hoffman RM, et al. Fluorophore-conjugated anti-CEA antibody for the intraoperative imaging of pancreatic and colorectal cancer. J Gastrointest Surg 2008; 12:1938-50; PMID: 18665430; DOI: 10.1007/s11605-008-0581-0.
12. Kojima T, Hashimoto Y, Watanabe Y, Kagawa S, Uno F, Kuroda S, et al. A simple biological imaging system for detecting viable human circulating tumor cells. J Clin Invest 2009; 119:3172-81; PMID: 19729837; DOI: 10.1172/JCI38609.
13. Mahooti S, Porter K, Alpaugh ML, Ye Y, Xiao Y, Jones S, et al. Breast carcinomatous tumoral emboli can result from encircling lymphovasculogenesis rather than lymphovascular invasion. Oncotarget 2010; 1:131-47; PMID: 21297224.
14. Runck LA, Kramer M, Ciraolo G, Lewis AG, Guasch G. Identification of epithelial label-retaining cells at the transition between the anal canal and the rectum in mice. Cell Cycle 2010; 9:3039-45; PMID: 20647777; DOI: 10.4161/cc.9.15.12437.
15. Uchugonova A, Hoffman RM, Weinigel M, Koenig K. Watching stem cells in the skin of living mice noninvasively. Cell Cycle 2011; 10:2017-20; PMID: 21558804; DOI: 10.4161/cc.10.12.15895.
16. Yamamoto N, Yang M, Jiang P, Xu M, Tsuchiya H, Tomita K, et al. Real-time imaging of individual fluorescent-protein color-coded metastatic colonies in vivo. Clin Exp Metastasis 2003; 20:633-8; PMID: 14669794; DOI: 10.1023/A:1027311230474.
17. Yamauchi K, Yang M, Jiang P, Xu M, Yamamoto N, Tsuchiya H, et al. Development of real-time subcellular dynamic multicolor imaging of cancer-cell trafficking in live mice with a variable-magnification whole mouse imaging system. Cancer Res 2006; 66:4208-14; PMID: 16618743; DOI: 10.1158/0008-5472.CAN-05-3927.

J Cancer Res Clin Oncol (2011) 137:1037–1051
DOI 10.1007/s00432-010-0969-6

ORIGINAL PAPER

Efficient virotherapy for osteosarcoma by telomerase-specific oncolytic adenovirus

Guidong Li · Hiroyuki Kawashima · Akira Ogose · Takashi Ariizumi · Yongjun Xu · Tetsuo Hotta · Yasuo Urata · Toshiyoshi Fujiwara · Naoto Endo

Received: 24 September 2010 / Accepted: 17 December 2010 / Published online: 31 December 2010

Abstract
Purpose A telomerase-specific oncolytic adenovirus, Telomelysin, can selectively kill cancer cells, and be attenuated in normal cells. We herein describe the oncolytic effect of Telomelysin on human osteosarcoma both in vitro and in vivo.
Methods The anti-tumor effects of Telomelysin were evaluated on human osteosarcoma cell lines in vitro and in a mouse xenograft model of human osteosarcoma in vivo. The replication efficiencies of Telomelysin in human osteosarcoma cell lines and normal cell lines and in osteosarcoma xenografts were determined by the expression levels of E1 mRNA and E1A protein using real-time quantitative PCR, Western blot analysis and immunohistochemistry. The in vitro telomerase-specific replication and the viral infection rate were also confirmed by TelomeScan (Telomelysin-GFP), using fluorescent microscopy and flow cytometry, respectively. The cell viabilities were examined by XTT assay, and the tumor volumes were measured every 2 days. The induction of apoptosis was assessed by Western blot analysis, as well as by TUNEL assay.
Results TelomeScan and Telomelysin were efficiently replicated in human osteosarcoma cell lines and led to a dose- and time-dependent expression of GFP, E1 mRNA and E1A protein. Telomelysin infection induced marked cytolysis and apoptosis in osteosarcoma cell lines in vitro. Neither cytotoxicity nor apoptosis were induced in normal human cell lines. In the human osteosarcoma cell xenograft model, intratumoral injection of Telomelysin resulted in increased viral replication, significant tumor growth suppression and distinct apoptotic cell death.
Conclusions This study indicated that virotherapy with Telomelysin may provide a promising strategy for the treatment of human osteosarcoma.

Keywords Osteosarcoma · Virotherapy · Oncolytic adenovirus · Telomerase · Apoptosis

G. Li · H. Kawashima (✉) · A. Ogose · T. Ariizumi · Y. Xu · T. Hotta · N. Endo
Division of Orthopedic Surgery, Graduate School of Medical and Dental Sciences, Niigata University, 1-757 Asahimachi-dori, Chuo-ku, Niigata 951-8510, Japan
e-mail: inskawa@med.niigata-u.ac.jp

G. Li
Department of Orthopedic Surgery, 2nd Affiliated Hospital of Harbin Medical University, 150086 Harbin, Heilongjiang, China

Y. Urata
Oncolys BioPharma Inc., Tokyo 106-0031, Japan

T. Fujiwara
Division of Surgical Oncology, Department of Surgery, Okayama University Graduate School of Medicine, Dentistry and Pharmaceutical Sciences, Okayama, Japan

T. Fujiwara
Center for Gene and Cell Therapy, Okayama University Hospital, Okayama 700-8558, Japan

Introduction

Osteosarcoma is the most frequent primary malignancy of bone, excluding multiple myeloma and is characterized by the production of immature bone by tumor cells. Osteosarcoma accounts for approximately 20% of primary bone sarcomas (Dorfman and Czerniak 1998) and about 75% of osteosarcoma occurs in children and adolescents (Horner et al. 2009). Despite many endeavors to improve the outcome of pre- and post-operative chemotherapy by

combining treatment with limb-salvaging surgery, the overall event-free survival rate has plateaued between 50 and 70% for non-metastatic high grade osteosarcoma patients (Goorin et al. 2003; Lewis et al. 2007), and the remaining approximately one-third of the patients do not benefit from these treatments. Furthermore, the current chemotherapeutic regimens are generally too aggressive and result in a broad spectrum of side effects (Sluga et al. 1999). These results indicate a dire need for more efficient and less toxic novel therapeutic modalities to increase the long-term survival of osteosarcoma patients.

Advances in knowledge regarding viral genomes and the molecular mechanism of viral infection and replication have led to the emergence of the conditionally replicating oncolytic adenovirus (CRAd) as a potential new approach for cancer therapy (Alemany and Curiel 2000; Kirn et al. 2001; Kirn 2001). One strategy to develop the CRAd is by altering viral genes so that viral replication restricted to only tumor cells. For example, a CRAd can be designed to have a deletion in the adenovirus early-region 1B (E1B) gene encoding a 55-kDa protein that binds and blocks p53 protein activity or to have a mutation in the converged region 2 (CR2) of the adenovirus E1A gene, leading the inability of the E1A protein to bind to the retinoblastoma protein (pRB; Chiocca 2002). ONYX-015 is an E1B-55-kDa gene-deleted CRAd, whose replication is restricted to tumor cells lacking normal p53 protein function, and which, in theory, cannot replicate in normal cells (Bischoff et al. 1996). Although deletion of the E1B-55-kDa protein confers some tumor specificity to the virus, the capacity of the virus to replicate and kill cells is markedly reduced, since the E1B-55-kDa protein is also important for the late phases of the viral life cycle (Leppard and Shenk 1989; Harada and Berk 1999). A CRAd with mutations in the pRB-binding region of the E1A protein would only replicate in tumor cells deficient in the p16/RB pathway (Fueyo et al. 2000). However, this type of virus was also shown to replicate and cause cell death in normal cells in vitro (Heise et al. 2000; Chiocca 2002). Another approach to design a form of CRAd is to develop a virus in which E1A gene transcription is under the control of a tumor marker-specific promoter, such as the prostate-specific antigen (Rodriguez et al. 1997) and E2F-1 genes (Tsukuda et al. 2002). The shortcoming of this type of CRAd is that it only replicates in cells exhibiting such tumor markers. Human telomerase and its catalytic subunit telomerase reverse transcriptase (hTERT) are activated in a large number of human cancers (~90%) regardless of tumor type, whereas their activities are silenced in normal somatic tissues (Kim et al. 1994; Shay and Bacchetti 1997). There has been evidence to suggest that controlling E1A gene expression under the hTERT promoter restricts adenoviral replication to telomerase-positive tumor cells and results in the efficient lysis of tumor cells (Wirth et al. 2003; Irving et al. 2004). We have therefore developed an oncolytic adenovirus (Telomelysin, OBP-301) in which the hTERT promoter controls the expression of E1A and E1B genes that are linked with an internal ribosome entry site (IRES; Kawashima et al. 2004). Our previous studies demonstrated that Telomelysin exhibits tumor-restricted replication and excellent cytotoxicity against many different types of cancers, but not of normal cells or tissues (Kawashima et al. 2004; Watanabe et al. 2006; Hashimoto et al. 2008; Hioki et al. 2008; Takakura et al. 2010). To the best of our knowledge, Telomelysin is the first hTERT-specific oncolytic adenovirus to be tested in a phase I clinical trial for various types of solid tumors.

Telomerase activation also frequently occurs in osteosarcoma and is correlated with decreased long-term survival (Ulaner et al. 2003; Sotillo-Piñeiro et al. 2004). We herein evaluated the viral replication efficacy and the anti-tumor effect of the telomerase-specific oncolytic adenovirus agent, Telomelysin in human osteosarcoma cell lines and a human osteosarcoma *nu/nu* mouse xenograft model.

Materials and methods

Cell lines and cell cultures

The human osteosarcoma cell lines, NOS1 and NOS10, were established in our laboratory as previously described (Hotta et al. 1992; Gu et al. 2004). The following human osteosarcoma cell lines were purchased from commercial sources: U2OS and SaOS2 from the American Type Culture Collection (ATCC, Bethesda, MD, USA), HuO9 from the Japan Cancer Research Resources Bank (JCRRB, Tokyo, Japan), HOS from the Institute for Fermentation (IFO, Osaka, Japan), MG-63 from the Health Science Research Resources Bank (HSRRB, Osaka, Japan), and OST from the Riken Cell Bank (RCB, Tsukuba, Japan). The human embryonic kidney cell line HEK-293 was purchased from the ATCC, the human cervical carcinoma cell line HeLa was obtained from RCB, the normal human dermal fibroblast cell line NHDF and the human mesenchymal stem cell line hMSC were purchased from Clonetics/Lonza Inc. (Walkersville, MD, USA). NOS-1, NOS-10, SaOS-2, HuO9, and OST cell lines were maintained in RPMI-1640 (Invitrogen, Carlsbad, CA, USA); U2OS, HeLa and HEK-293 were cultured in DMEM (Invitrogen); and the HOS and MG-63 were cultured in α-MEM (Invitrogen). All media were supplemented with 10% FBS (PAA Laboratories GmbH, Pasching, Austria) containing 1% antibiotics and anti-mycotics (Invitrogen). The NHDF cell lines were cultured in fibroblast basal medium supplemented with 2% fetal bovine serum, 0.1%

insulin, 0.1% human fibroblast growth factor B, 0.1% gentamicin sulfate and 0.1% amphotericin B (FGM-2 BulletKit, Clonetics/Lonza). The hMSC cell lines were cultured in MSC basal medium supplemented with MSC Growth Supplement, L-glutamine, and 0.1% gentamicin sulfate and 0.1% amphotericin B (MSCGM BulletKit, Clonetics/Lonza). All cell cultures were incubated at 37°C, in an atmosphere of 5% CO_2 with 100% humidity.

Recombinant adenovirus

Telomelysin (OBP-301) is a recombinant telomerase-specific replication-selective type 5 adenovirus, in which the expression of the E1A and E1B genes linked by an internal ribosome entry site (IRES) is under the control of the hTERT promoter. TelomeScan (Telomelysin-GFP; OBP-401) is a telomerase-specific replication-competent adenovirus variant, in which the green fluorescent protein (GFP) gene under the control of the cytomegalovirus promoter is inserted into the deleted E3 region of Telomelysin (OBP-301) for monitoring viral replication. The construction and features of Telomelysin and TelomeScan have been described in detail in previous studies (Kawashima et al. 2004; Umeoka et al. 2004; Fujiwara et al. 2006; Kishimoto et al. 2006). The E1A-deleted replication-deficient adenovirus, d1312, was used as a control vector. The viruses were purified using $CsCl_2$ linear gradient ultracentrifugation. Viral titers were determined using a plaque-forming assay on HEK-293 cells.

Real-time quantitative reverse-transcriptase PCR

The mRNA expression of hTERT was examined in cultured non-infected cell lines including 8 human osteosarcoma cell lines (NOS1, U2OS, HuO9, SaOS2, HOS, MG-63, OST and NOS10), 1 normal human fibroblast cell line (NHDF) and 1 human mesenchymal stem cell line (hMSC). Three osteosarcoma cell lines (NOS10, SaOS2 and HuO9) and two normal cell lines (NHDF and hMSC) were chosen for Telomelysin infection. The cells (5×10^5) were seeded on 6-cm culture dishes 24 h before viral infection and were then infected with Telomelysin at a multiplicity of infection (MOI) of 0.1 and 1 or with replication-deficient adenovirus d1312 at a MOI of 1. The viral replication capacity was tested by measuring adenovirus E1A and E1B gene expression levels at 24, 48 and 72 h after Telomelysin infection. Total RNA was extracted using the Isogen Reagent (Nippongene, Toyama, Japan), and the mRNA expression was examined by real-time quantitative reverse-transcriptase PCR (qRT-PCR), as described previously (Li et al. 2009). Briefly, reverse transcription was carried using the PrimeScript RT reagent kit (Takara Bio, Tokyo, Japan), according to the manufacturer's protocol. Real-time PCR was performed using the Thermal Cycler Dice Real Time System (Takara) and the SYBR Premix Ex Taq II (Perfect Real Time) PCR kit (Takara) according to the manufacturer's instructions. The primer sequences used in this study were as follows: hTERT, 5′-GAGTGTCTGGAGCA AGTTGCAAAG-3′ (forward) and 5′-CACGACGTAGT CCATGTTCACAATC-3′ (reverse); E1A, 5′-GTATGAT TTAGACGTGACGG-3′ (forward) and 5′-GATAGCA GGGCGCATTTTAG-3′ (reverse); E1B, 5′-GGCTAAAG GGGGTAAAGAGGG-3′ (forward) and 5′-CCTTACA TCGGTCCAGGCTTC-3′ (reverse); GAPDH, 5′-GCA CCGTCAAGGCTGAGAAC-3′ (forward) and 5′-TGGT GAAGACGCCAGTGGA-3′ (reverse). The DNA amplification program for the hTERT genes consisted of denaturation at 95°C for 10 s, followed by 40 cycles of denaturation at 95°C for 5 s, and annealing and extension at 60°C for 30 s. PCR amplification of the E1A and E1B genes consisted of denaturation at 95°C for 10 s followed by 40 cycles of denaturation at 95°C for 30 s, annealing at 55°C for 30 s, and extension at 72°C for 1 min. Data were analyzed using the Thermal Cycler Dice Real Time System analysis software package (Takara). The HeLa cell line was known to be positive for hTERT expression and was used as a positive control (Meyerson et al. 1997). HEK-293 cell lines were used as a positive control for E1A and E1B gene expression, since this cell line is known as an adenovirus 5 DNA-transformed cell line. The PCR results were normalized to those of the housekeeping gene GAPDH, and the relative level of expression of each mRNA was calculated by dividing the level of the mRNA expression of the sample by the level of the positive control (which was assigned a value of 1). Each value was expressed as the mean ± SD of quadruplicate separate experiments.

Fluorescence microscopy

To visualize the hTERT-selective viral replication in vitro, 3 human osteosarcoma cell lines (NOS10, SaOS2 and HuO9) and 2 normal cell lines (NHDF and hMSC) were seeded on Lab-Tek chamber slides (Nalge Nunc International, Rochester, NY, USA) at a density of 1.25×10^5 cells/well 24 h before viral infection. The cells were infected with TelomeScan (Telomelysin-GFP) at MOIs of 1 and 10, and the cells were treated with PBS as a control. GFP fluorescence was detected and photographed (magnification: 100×) under an Olympus BX-50 bright-field microscope equipped with BX-FLA fluorescence attachment using a NIBA filter (excitation, 470–490 nm; emission, 515–550 nm).

Flow cytometric analysis

To assess the viral infection rate of Telomelysin, 5×10^5 cells (NOS10, SaOS2, HuO9, NHDF and hMSC) were

seeded on 6-cm dishes 24 h before infection and were then infected with TelomeScan (Telomelysin-GFP) at MOIs of 0, 0.1, 1 and 10. At 48 h after infection, the cells (containing floating cells) were harvested, washed twice with FACS buffer (5% FBS in PBS, 1 mM EDTA) and resuspended in FACS buffer. The percentage of GFP-positive cells was analyzed using a BD FACSCalibur flow cytometer and the CellQuest pro software package (Becton–Dickinson; Franklin Lakes, NJ, USA). A minimum of 10,000 events were examined for each experiment.

Western blot analysis

After the cells were infected with Telomelysin, the protein expression of E1A was assessed using a mouse anti-Adenovirus type 5 E1A monoclonal antibody (1:3,000; BD Biosciences PharMingen, San Diego, CA, USA). The induction of apoptosis was detected by the expressions of cleaved caspase 3 and poly (ADP-ribose)-polymerase (PARP) proteins using rabbit anti-caspase 3 and anti-PARP (1:1,000; Cell Signaling Technology, Beverly, MA, USA), respectively. In addition, activation of autophagy was examined by the expression of microtubule-associated protein 1 light chain 3 (LC3-I and II) proteins using anti-LC3B polyclonal antibodies (1:1,000; Cell Signaling Technology). The expression of the β-actin protein was detected by a mouse anti-β-actin monoclonal antibody (1:3,000; Sigma–Aldrich St. Louis, MO, USA), and used as an internal control. The cells were washed twice with ice-cold PBS and 100 µl of sample buffer (62.5 mM Tris pH 6.8, 2% SDS, 5% glycerol, 6 M urea), and 4 µl of a protease inhibitor cocktail (Complete, Roche Diagnostic GmbH, Mannheim, Germany) was added to each 6-cm dish. Cell lysates were collected on ice, microcentrifuged at 4°C for 5 min, and the protein concentrations of the supernatants were measured using the BCA protein assay kit (Pierce, Rockford, IL, USA). The supernatants were mixed with 5% (v/v) of 1 M dithiothreitol and 5% (v/v) of bromophenol blue and were heated at 95–100°C for 5 min. Equal amounts (50 µg) of proteins were separated by SDS–PAGE gels (7.5–15% acrylamide) and then electro-transferred to nitrocellulose membranes. The membranes were incubated with the primary antibodies indicated earlier, followed by probing with horseradish peroxidase-linked donkey anti-rabbit or sheep anti-mouse IgG (Amersham Biosciences, Buckinghamshire, UK), and they were then developed using ECL detection reagents (Amersham Biosciences). The blots were re-probed with an anti-β-actin antibody to ensure uniform sample loading.

Cell viability assay

The human osteosarcoma cell lines (NOS10, SaOS2 and HuO9) and normal cell lines (NHDF and hMSC) were plated on 96-well plates at a density of 5×10^3 cells/well 24 h before Telomelysin infection. NOS10, SaOS2 and HuO9 cells were infected with Telomelysin at MOIs of 0.01, 0.1, 1, 2 or 5; NHDF and hMSC cells were infected with Telomelysin at MOIs of 0.01, 0.1, 1, 5 or 10. As a control, cells were also infected with PBS (mock) or d1312 (MOI of 1). Cell viability was assessed by the XTT (sodium 3′-[1-(phenylaminocarbonyl)-3,4-tetrazolium]-bis (4-methoxy-6-nitro) benzene sulfonic acid hydrate) assay 72 h after viral infection using the Cell Proliferation Kit-II (Roche Diagnostics, Indianapolis, IN, USA) according to the manufacturer's protocol, except for the normal cell lines (NHDF and hMSC), which were assessed 7 days after infection. For other experiments, the osteosarcoma cell lines (NOS10, SaOS2 and HuO9) and normal cell lines (NHDF and hMSC) were plated on 6-cm dishes at a density of 5×10^5 cells/dish 24 h before viral infection and were then infected with Telomelysin at a MOI of 1 for osteosarcoma cell lines or at a MOI of 10 for normal cell lines. Cells treated with PBS (mock) were used as controls. Cell morphology was observed daily using an Olympus phase-contrast microscope ULWCD 0.30 (IMT2, Olympus, Tokyo, Japan), and photomicrographs were taken at 72 h and 7 days after infection for osteosarcoma cell lines and normal cell lines, respectively, using the Olympus DP12 digital camera attached to the microscope (magnification, ×40).

In vivo tumor growth

Human osteosarcoma cell line NOS10 (1×10^7 cells/mouse) were implanted subcutaneously into the flanks of 6-week-old female BALB/c *nu/nu* mice. When tumors reached 5–6 mm in diameter, the mice were randomly divided into 3 groups ($n = 6$ for each group) and were injected intratumorally with 50 µl of a solution containing 1.0×10^7 plaque-forming units (pfu) of Telomelysin, the replication-deficient control adenovirus d1312, or PBS, on days 1, 2 and 3. The perpendicular diameters of the tumors were measured using micrometer calipers every 2 days, and the tumor volume (mm^3) was calculated using the following formula: tumor volume (mm^3) $= 0.5 \times a \times b^2$, where a and b are the longest and the shortest diameters, respectively. The experiments were approved by the Ethics Review Committee for Animal Experimentation of Niigata University, Graduate School of Medical and Dental Sciences.

In vivo viral replication

PBS, d1312 or Telomelysin (1.0×10^7 pfu/mouse) was injected intratumorally into NOS10 tumor-bearing BALB/c *nu/nu* mice. At 1, 2 weeks and 1 month after the last viral injection, the animals were euthanized under deep isoflurane anesthesia and the xenografted tumors were harvested to prepare total RNA. Viral replication was determined by the level of E1A and E1B mRNA expression using real-time qRT-PCR, as described earlier.

Immunohistochemical staining and TUNEL assay

At 1, 2 weeks and 1 month after intratumoral administration of PBS, d1312 or Telomelysin, the tumors were harvested, fixed in 4% paraformaldehyde and embedded in paraffin. Tumor tissue sections (4 μm) were subjected to hematoxylin and eosin (HE) staining for histopathological evaluation. To assess viral replication and lateral spread, paraffin-embedded tumor sections were deparaffinized and subjected to immunohistochemical staining. An anti-adenovirus type 5 E1A antibody (1:50, BD Biosciences) was used as the primary antibody, and a Histofine Simple Stain PO (MULTI) kit (Nichirei, Tokyo, Japan) was used as the secondary antibody according to the manufacturer's protocol. Signals were detected using 3,3-diaminobenzidine (DAB, Nichirei) and were counterstained with hematoxylin. Cell block sections of HEK-293 were used as a positive control. Apoptotic cell death was detected using the terminal deoxynucleotidyl transferase-mediated dUTP nick-end labeling (TUNEL) assay and an In situ Apoptosis Detection Kit (Takara) according to the manufacturer's protocol. The tumor sections were then counterstained with hematoxylin. Cell block sections of HeLa cell line that were serum-starved (cultured cells were rinsed with PBS and were then maintained in serum free DMEM overnight) or that were cultured in nutrient-rich medium (DMEM with 10% FBS) were used as positive and negative controls, respectively. Cell images were captured using an Olympus DP-50 digital camera Viewfinder Lite 1.0 system and were processed using the Studio Lite software package (Olympus).

Statistical analysis

Data are shown as the means ± SD. The statistical significance of differences between groups was evaluated using a two-tailed Student's *t*-test and the Microsoft Excel program. A *P*-value of less than 0.01 signified statistical significance.

Results

Expression of hTERT in human osteosarcoma cell lines and in normal cell lines

To determine whether human osteosarcoma cell lines might be good targets for Telomelysin infection, we assayed the expression level of hTERT mRNA by real-time qRT-PCR analysis. All human osteosarcoma cell lines tested (8/8) expressed detectable levels of hTERT mRNA (Fig. 1), although the expression levels varied. In contrast, the NHDF and hMSC cell lines were negative for hTERT mRNA expression. The relative level of hTERT mRNA expression was high in osteosarcoma cell lines MG63, OST, NOS10 and HOS (ranging from 1.69 to 51.1), and somewhat lower in osteosarcoma cell lines HuO9, NOS1, U2OS and SaOS2 (ranging from 0.11 to 0.23), compared with levels in the control cell line, HeLa. The highest relative level of hTERT mRNA expression was in the HOS (51.1) and the lowest was in HuO9 (0.11).

Replication efficiency of Telomelysin in human osteosarcoma and normal cell lines

To assess the adenovirus replication capacity, 3 human osteosarcoma cell lines and 2 two normal cell lines were infected with d1312 or Telomelysin at a MOI of 0.1 or 1, and the adenovirus E1A and E1B mRNA expression, and E1A protein expression, were detected at 24, 48 and 72 h after infection. Telomelysin infection induced marked expression of E1A and E1B mRNA in the osteosarcoma

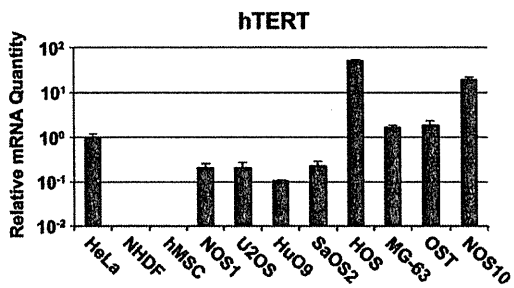

Fig. 1 Expression of hTERT in human osteosarcoma cell lines and normal human cell lines. Expression of hTERT mRNA in human osteosarcoma cell lines (NOS1, U2OS, HuO9, SaOS2, HOS, MG63, OST and NOS10), in normal human dermal fibroblast (*NHDF*) and in a human mesenchymal stem cell line (*hMSC*) were measured by real-time quantitative RT-PCR analysis using specific primers for hTERT. The relative level of mRNA expression was normalized using the expression of the housekeeping gene, GAPDH, in each cell line, and the values were calculated relative to that of the positive control HeLa cell line, which was assigned a value of 1. Each sample was tested at least in triplicate, and the data represent the means ± SD

cell lines (HuO9, SaOS2 and NOS10) in a dose- and time-dependent fashion, and the expression level of E1A and E1B mRNA seemed to correlate linearly with their hTERT expression levels (lower, medium and high expression, respectively) (Fig. 2a). The expression of E1A and E1B mRNA was also detected in normal cell lines NHDF and hMSC, the expression level, however, was very low when compared with those of the osteosarcoma cell lines we tested. When Telomelysin was infected at a MOI of 1 for 72 h, the values of the fold-increases in E1A and E1B mRNA expression in NOS10, SaOS2 and HuO9 cell lines were 133 and 44, 41 and 22, and 12 and 4, respectively, compared to the expression levels in the NHDF cell line, and were 9,685 and 43,596, 2,792 and 850, and 850 and 420, respectively, compared to the expression levels in the hMSC cell line (Fig. 2a). The cell lines treated with d1312 showed no detectable E1A mRNA expression, in spite of their extremely low level of E1B mRNA expression (at least 1,500-fold lower than control cell line) (Fig. 2a). To further confirm the replication efficiency and specificity of Telomelysin at the protein level, a Western blot analysis of adenovirus E1A protein expression was also performed. Consistent with the E1A and E1B mRNA expression levels, the E1A protein expression was also increased in a time- and dose-dependent manner in the osteosarcoma cell lines (NOS10, SaOS2 and HuO9) infected with Telomelysin (Fig. 2b). Low level of E1A protein expression was also detected in NHDF cell lines but could not be detected in hMSC cell lines (Fig. 2b). Densitometric quantification of the protein bands showed that Telomelysin infection at a MOI of 1 for 72 h resulted in an approximately 2.8-, 1.9- and 1.2-fold increase in the E1A protein signal in NOS10, SaOS2 and HuO9, respectively, compared with the signal in NHDF (Fig. 2c). None of the cell lines had detectable expression of the E1A protein when infected with d1312.

Telomerase-selective viral replication in vitro visualized by TelomeScan

To confirm the hTERT promoter selectivity of Telomelysin, we infected osteosarcoma cell lines (NOS10, SaOS2 and HuO9) and normal cell lines (NHDF and hMSC) with TelomeScan, a genetically modified Telomelysin expressing GFP, and green fluorescence was observed by fluorescence microscopy. As shown in Fig. 3a, osteosarcoma cell line NOS10 expressed gradually increasing bright green fluorescence in a dose-, and a time-dependent manner after TelomeScan infection at a MOI of either 1 or 10. The GFP expression level in NOS10 could be detected as early as in 12 h after TelomeScan infection at a MOI of 1, and the fluorescence intensity was attenuated at 96 h after infection due to the severe cell death induced by TelomeScan. In SaOS2 and HuO9, we also observed a dose-, and a time-dependent GFP expression. The earliest expression of GFP in these two cell lines were at 12 and 24 h after TelomeScan infection at a MOI of 10 (figures are not shown). In contrast, the normal NHDF cell lines (Fig. 3a) and the normal hMSC cell lines (figure is not shown) exhibited only sporadic fluorescence in a few cells even at a MOI of 10 at 96 h after TelomeScan infection.

We also determined the viral infection rate of TelomeScan by quantifying the GFP expression using flow cytometric analysis. The GFP expression was also gradually increased in a dose-dependent manner in the osteosarcoma cell lines NOS10, SaOS2 and HuO9, whereas the normal cell lines NHDF and hMSC exhibited very low levels of GFP expression. The percentages of GFP expression in the NOS10, SaOS2 and HuO9 were 92.2 and 99.2, 82.2 and 98.6, and 64.3 and 88.4%, respectively, at MOI 1 and MOI 10 (Fig. 3b). In contrast, the expressions of GFP in NHDF and hMSC were only 7.8 and 19.0, 1.63 and 3.21%, respectively, at MOI 1 and MOI 10 (Fig. 3b).

In vitro cytotoxic effects of Telomelysin on human osteosarcoma cell lines

To examine the selective cytotoxic effect of Telomelysin, NOS10, SaOS2, HuO9, NHDF and hMSC cell lines were mock-infected (PBS), infected with d1312 or infected with Telomelysin at the indicated MOIs. Cell viability was assessed at 72 h after infection using the XTT assay, except for NHDF and hMSC, which were evaluated at 7 days after infection because of their slower rate of growth. As shown in Fig. 4a, Telomelysin infection was highly cytotoxic to the 3 osteosarcoma cell lines in a dose-dependent fashion, even at a MOI of 0.1. Approximately 20–90% of the NOS10 cells, 12–78% of the SaOS2 cells and 14–60% of the HuO9 cells were killed by Telomelysin infection at MOIs ranging from 0.1 to 5, respectively, compared with mock-infected cells, and these differences in values were significant ($P < 0.01$). In contrast, no cytotoxic effect was observed in normal cell lines NHDF and hMSC after infection with Telomelysin, even at the high concentration of MOI of 10, at 7 days after infection. In addition, no clear cytotoxic effect could be detected in any d1312 infected cell lines. Photomicrographs of cells taken using phase-contrast microscopy also demonstrated that 72 h after Telomelysin infection at a MOI of 1, distinct cell death, evidenced by a mass of rounded up, floating, highly refractile cells, was induced in NOS10, SaOS2 and HuO9 cell lines (Fig. 4b). However, no cell lysis was observed in the NHDF cell lines and hMSC cell lines even at 7 days after infection with Telomelysin at a MOI of 10.

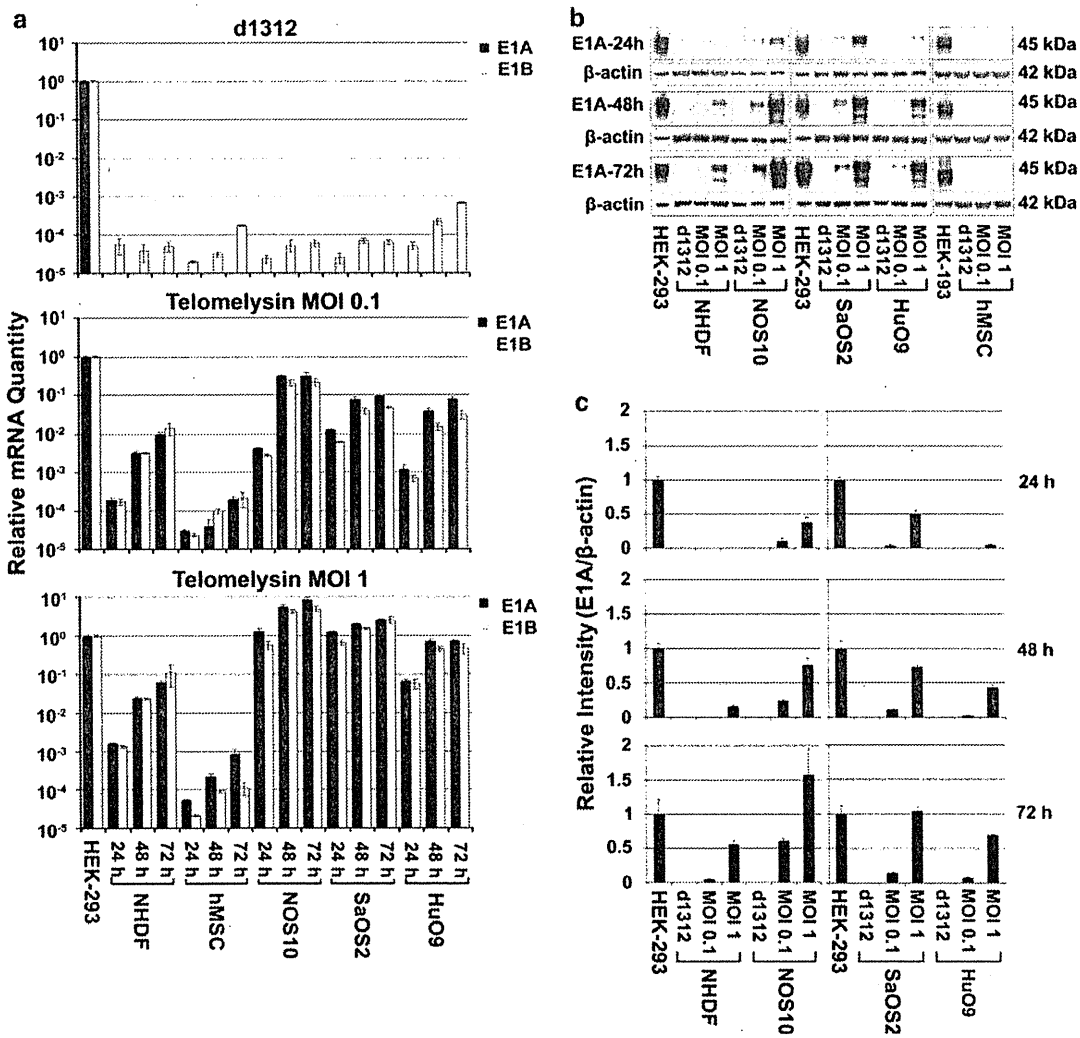

Fig. 2 Adenovirus E1A, E1B gene and E1A protein expression levels after Telomelysin infection in human osteosarcoma cell lines and normal cell lines. The human osteosarcoma cell lines (NOS10, SaOS2 and HuO9), normal cell lines (NHDF and hMSC) or the control HEK293 cell lines were infected with d1312 at a MOI of 1 or with Telomelysin at a MOI of 0.1 or 1. The cells were harvested 24, 48 and 72 h after infection, and the viral replication rate was determined by the measurement of the E1A and E1B mRNA and E1A protein expression using real-time qRT-PCR (**a**) and a Western blot analysis (**b**), respectively. The mRNA expression levels were normalized to the expression of human GAPDH. The mRNA expression levels of E1A and E1B of HEK-293 were assigned a value of 1, and the mRNA expression of each cell line was calculated relative to that of HEK-293 cell lines. Data are presented as the means ± SD values of three separate experiments. Equivalent amounts of protein from cell lysates were separated on SDS–PAGE and were then probed with anti-adenovirus type 5 E1A and anti-β-actin antibodies. **c** The intensity of each protein band in the gel was quantified by densitometric scanning using the NIH-Image J software package, and each value was normalized to the β-actin signal. The intensity of the HEK-293 signal was assigned a value of 1.0. Intensities relative to those of HEK-293 are presented as the means ± SD of triplicate measurements

In vitro induction of apoptotic cell death by Telomelysin infection in human osteosarcoma cell lines

To determine the mechanism responsible for the significant cell death in osteosarcoma cell lines (NOS10, SaOS2 and HuO9) induced by Telomelysin infection in vitro, apoptosis and autophagy were examined by a Western blot analysis. Activation (cleavage) of caspase-3 plays a critical role in the execution of apoptosis (Fernandes-Alnemri et al. 1994), and the proteolytic cleavage of PARP by activated caspase-3 serves as a marker of apoptosis (Oliver et al. 1998). Similarly, the conversion of a cytosolic LC3-I to an autophagosome-associating form, LC3-II, has been used as an indicator of autophagy (Kabeya et al. 2004). Thus, the present study examined the induction of apoptosis or

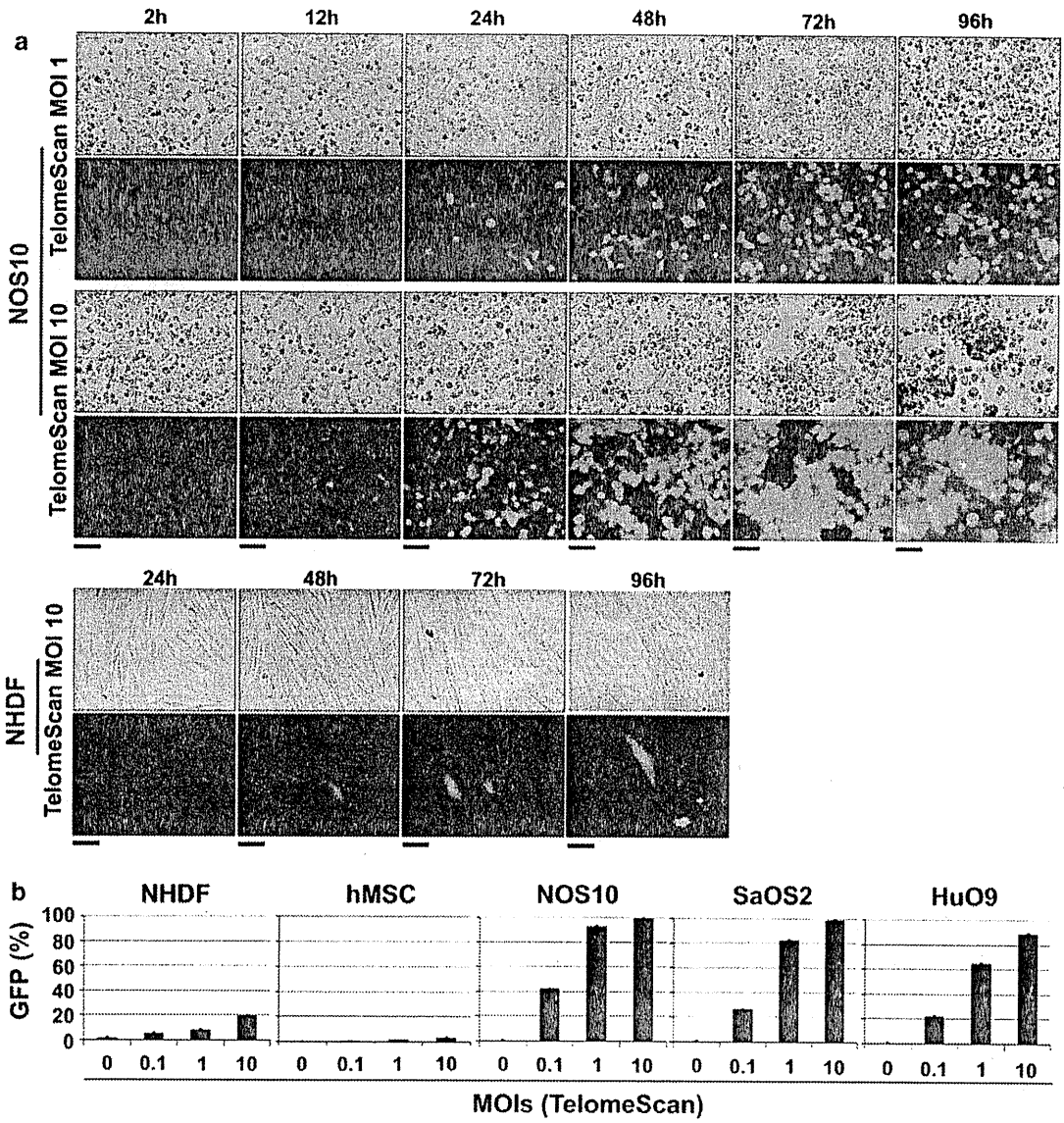

Fig. 3 **a** Selective visualization of human osteosarcoma cell lines using the telomerase-specific, replication-competent adenovirus TelomeScan. The cells were infected with TelomeScan (modified Telomelysin expressing GFP) at a MOI of 1 or a MOI of 10 for NOS10 and at a MOI of 10 for NHDF. Cell morphology was observed under a light microscope (*top panels*), and GFP fluorescence was detected and photographed under fluorescent microscope (*bottom panels*) at the indicated time points. Original magnification, ×200; scale bar, 50 μm. **b** The infectivity of TelomeScan in human osteosarcoma cell lines and normal cell lines. NOS10, SaOS2, HuO9, NHDF and hMSC cells were infected with TelomeScan at MOIs of 0, 0.01, 1 or 10, then the percentage of GFP expression was analyzed by a FACSCalibur flow cytometer 48 h post-infection. Data are representative of three separate experiments

autophagy by detection of the cleavages of caspase 3 and PARP protein expression, and by changes in the ratio of LC3B-II/I protein expression, respectively. At 72 h after Telomelysin infection, obvious dose-dependent cleavages of caspase 3 and PARP were observed in all 3 osteosarcoma cell lines (Fig. 5a), whereas no caspase activation was detected in the normal NHDF cell lines. However, there was no increase in the level of LC3B-II, a marker of autophagy, in either the osteosarcoma cell lines or in the NHDF cell lines infected with Telomelysin (Fig. 5b).

The oncolytic effect of intratumoral infection of Telomelysin on human osteosarcoma tumor xenografts.

To examine the oncolytic effect of Telomelysin on human osteosarcoma in vivo, *nu/nu* mice bearing NOS10 tumors were administered three consecutive daily intratumoral injections of 1×10^7 pfu/body of Telomelysin,

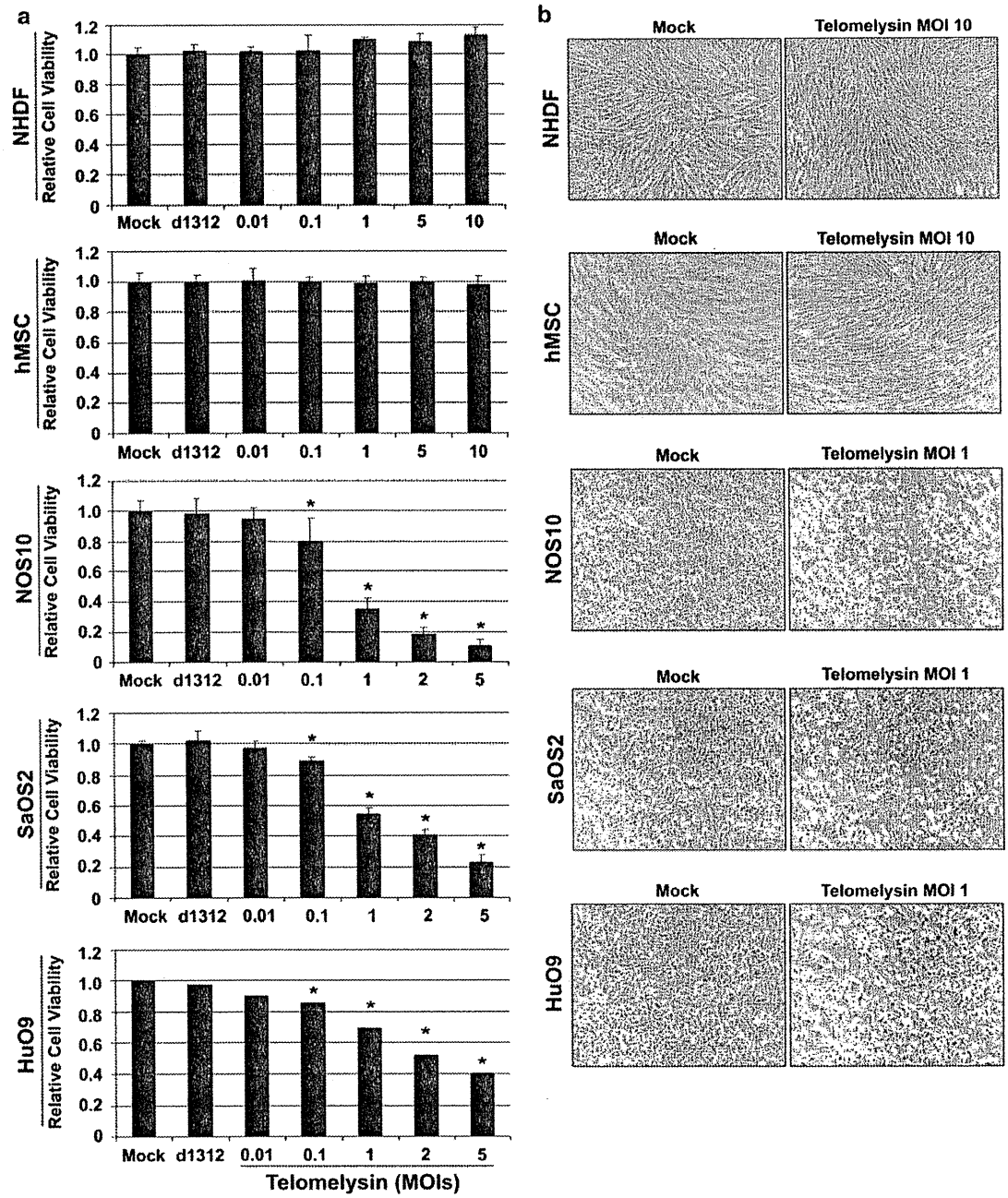

Fig. 4 Cell-killing effect of Telomelysin on human osteosarcoma cell lines. **a** NOS10, SaOS2 and HuO9 cell lines were infected with Telomelysin at MOIs of 0.01, 0.1, 1, 2 and 5; NHDF and hMSC cell lines were infected with Telomelysin at MOIs of 0.01, 0.1, 1, 5 and 10. Cells treated with PBS (mock) or infected with d1312 were used as controls. The cell viability was determined using an XTT assay 72 h after infection, except for the NHDF and hMSC cell lines, which were assessed at 7 days post-infection. The cell viability of the mock-infected cells was regarded as 1.0, and the relative cell viability of each cell line was calculated compared to that of mock-infected cells. Data are depicted as the means ± SD values of quadruple experiments. Differences among groups were analyzed using the Student's *t*-test. Statistical significance (*) was defined as $P < 0.01$, when Telomelysin was compared with mock or d1312-infected cells. **b** Photomicrographs of human osteosarcoma cell lines and normal cell lines after Telomelysin infection. Cell morphologies of NOS10, SaOS2, HuO9, NHDF and hMSC Cell lines were observed using a phase-contrast microscope and were photographed at a magnification of ×40, at 72 h after viral infection except NHDF and hMSC, which were photographed 7 days after infection

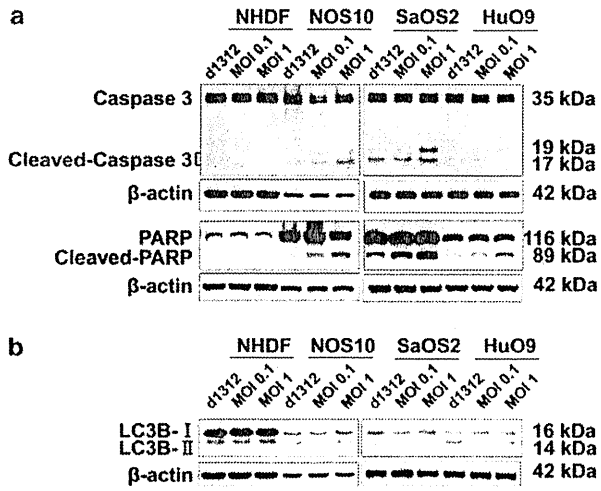

Fig. 5 Telomelysin induced apoptosis but not autophagy in human osteosarcoma cell lines in vitro. NOS10, SaOS2, HuO9 and NHDF cell lines were infected with d1312 at a MOI of 1 or were infected with Telomelysin at a MOI of 0.1 or 1 and were harvested at 72 h after infection. Equal amounts of protein from cell lysates were separated on SDS–PAGE gels for a Western blot analysis of cleaved caspase 3, cleaved PARP (**a**) and LC3B-I and LC3B-II (**b**), as markers of apoptosis and autophagy, respectively. *Each blot* was reprobed with an anti-β-actin antibody to confirm uniform loading

d1312 or PBS. Macroscopic analysis of the tumors indicated that the tumor size following Telomelysin infection was markedly smaller than in mock- or d1312-treated tumors (Fig. 6a). Tumor growth was significantly inhibited following Telomelysin infection from day 15 to day 31 ($P < 0.01$) compared to PBS- or d1312-treated tumors, and no tumor suppression was detected in the d1312-treated tumors (Fig. 6b).

Efficient in vivo replication and apoptosis induction of Telomelysin in tumor tissues

To evaluate the replication efficiency of Telomelysin in vivo, adenovirus E1A and E1B mRNA expression in the implanted NOS10 tumors was analyzed by real-time qRT-PCR. Tumor xenograft-bearing mice were administered three consecutive daily intratumoral injections of 1×10^7 pfu of Telomelysin, d1312, or the PBS control, and the tumors were harvested 1, 2 weeks and 1 month after treatment. Consistently high levels of E1A and E1B mRNA expression were detected at 1 and 2 weeks after Telomelysin infection, with approximately 1.3- and 1.0-fold, and 1.5- and 2.1-fold expression, respectively, compared to that in HEK-293 cell lysates (assigned a value of 1.0). At 1 month after viral infection, the E1A and E1B mRNA expression of Telomelysin was still detectable, although the expression levels were reduced by approximately four and fivefold compared to those of HEK-293 cell lysates (Fig. 6c). However, no E1A or E1B mRNA expression was detected in PBS- or d1312-treated tumors except for extremely weak E1B expression in d1312-infected tumors at 1 and 2 weeks after viral infection.

To further evaluate the replication and lateral spread of Telomelysin in NOS10 tumor xenografts, histological analysis and immunohistochemical staining of adenovirus E1A were performed at 1, 2 weeks and 1 month after the last viral injection. A standard HE stain showed that Telomelysin infection induced increasing tumor cell death over time that was characterized by a high level of nuclear condensation and was accompanied by massive intratumoral hemorrhage 1 and 2 weeks after infection (Fig. 7j, k). However, by 1 month after Telomelysin infection, almost all of the tumor cells had been eradicated and were replaced by suffusive hemorrhage and hemosiderin deposition. Detectable dead tumor cells were mainly peripherally restricted to the borders of the small tumor remnant (Fig. 7l). In contrast, no clear cell death was detected in PBS-treated tumors except for a few dead cells that were located in the area of intratumoral hemorrhage. In addition, an osteoid matrix could be observed 1 month after treatment in the PBS-treated tumors (Fig. 7a–c). Immunohistochemical staining revealed that the expression of the E1A protein increased over the first 2 weeks in Telomelysin-treated tumor sections. E1A protein staining was heterogeneous at 1 week, and became more diffuse at 2 weeks after Telomelysin infection (Fig. 7m and n). However, at 1 month after viral infection, the E1A expression had almost completely disappeared, except for faint expression that could be detected in the peripheral tumor remnant (Fig. 7o). In contrast, no E1A protein was detected in tumors that were treated with PBS for more than 1 month (Fig. 7d–f).

To confirm that apoptosis contributes to the Telomelysin-mediated tumor cell death in the mouse xenograft model, TUNEL assays were performed using paraffin-embedded tumor sections. Treatment with Telomelysin clearly induced an increase in the number of TUNEL-positive tumor cells detected in tumor sections. These apoptotic tumor cells stained patchily or focally at 1 week after infection, but their staining was more uniform and diffuse at 2 weeks after Telomelysin infection (Fig. 7p and q). These TUNEL-positive cells showed a strong linear correlation with the large numbers of intracellular viral genomes. However, TUNEL-positive tumor cells were only detected in some, but not all, of the borders and inner areas of peripheral tumor remnants (Fig. 7r). There was no evident apoptotic cell death in the tumors treated with PBS for more than 1 month (Fig. 7g–i).

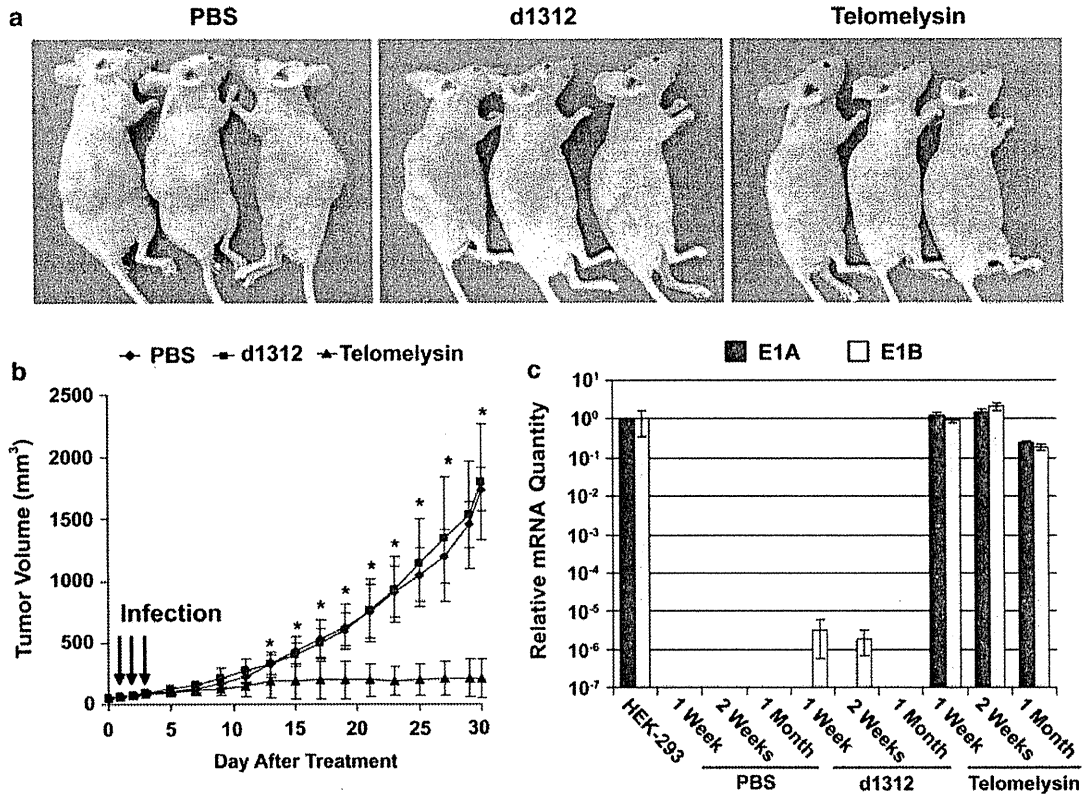

Fig. 6 Tumor growth inhibition and viral replication induced by Telomelysin infection in *nu/nu* mice bearing human osteosarcoma cell xenografts. Human osteosarcoma NOS10 cells (1×10^7 cells/mouse) were injected subcutaneously into the flanks of BALB/c *nu/nu* mice, and Telomelysin (1×10^7 pfu/mouse) was administered intratumorally daily for three consecutive days. PBS- and replication-deficient adenovirus d1312 were used as controls. Six mice were used for each group. **a** Gross appearances of the NOS10 xenografted tumors in *nu/nu* mice at 1 month after Telomelysin infection. **b** Tumor growth is depicted as the mean tumor volume ± SD, and statistical significance (*) was defined as $P < 0.01$ (Student's *t*-test). (c) NOS10 tumor-bearing mice received daily intratumoral injection of PBS, d1312 or Telomelysin (1×10^7 pfu/body) for 3 days. The viral yield of each subcutaneous tumor was determined by E1A and E1B mRNA expression levels using real-time quantitative RT-PCR at 1, 2 weeks and 1 month post-infection. The results were normalized to the level of human GAPDH. The relative level of E1A and E1B mRNA expression for each group was defined as the fold increase relative to that of HEK-293 mRNA expression (the expression level in HEK-293 cell lines was assigned a value of 1). Data are shown as the means ± SD of quadruplicate separate experiments

Discussion

Telomelysin (OBP-301), a telomerase-specific replication-selective adenovirus, has been shown to induce notable tumor-targeted oncolysis in a broad range of human cancers (Kawashima et al. 2004; Watanabe et al. 2006; Hashimoto et al. 2008; Hioki et al. 2008; Takakura et al. 2010), and a phase I trial in patients with advanced solid tumors is currently in progress (Fujiwara et al. 2008). In this study, we showed for the first time that this novel potential anti-tumor adenovirus, Telomelysin, induces apoptotic cell death-mediated oncolysis in human osteosarcoma both in vitro and in vivo.

The up-regulated transcriptional activity of hTERT is essential for immortalization and cancer development (Takakura et al. 1999). Activation of hTERT is also a frequent phenomenon in osteosarcoma and correlates with an unfavorable prognosis (Scheel et al. 2001; Ulaner et al. 2003). In this study, hTERT mRNA expression was detected in all eight of the human osteosarcoma cell lines we tested, whereas it could not be detected in a normal human fibroblast cell line or normal human mesenchymal stem cell line (Fig. 1). We assessed the tumor-specific transcriptional activity of the hTERT promoter in hTERT-positive osteosarcoma cell lines, normal human fibroblast and normal human mesenchymal stem cell lines following Telomelysin infection in vitro. A dose- and time-dependent efficient viral replication assessed by increased expression of both the E1 gene (Fig. 2a) and the E1A protein (Fig. 2b and c) was observed in all of the osteosarcoma cell lines we tested. In contrast, normal cell lines showed a very low level of expressions of the E1 gene and E1A protein. Selective visualization of viral infectivity of human osteosarcoma cells by TelomeScan also exhibited a dose- and

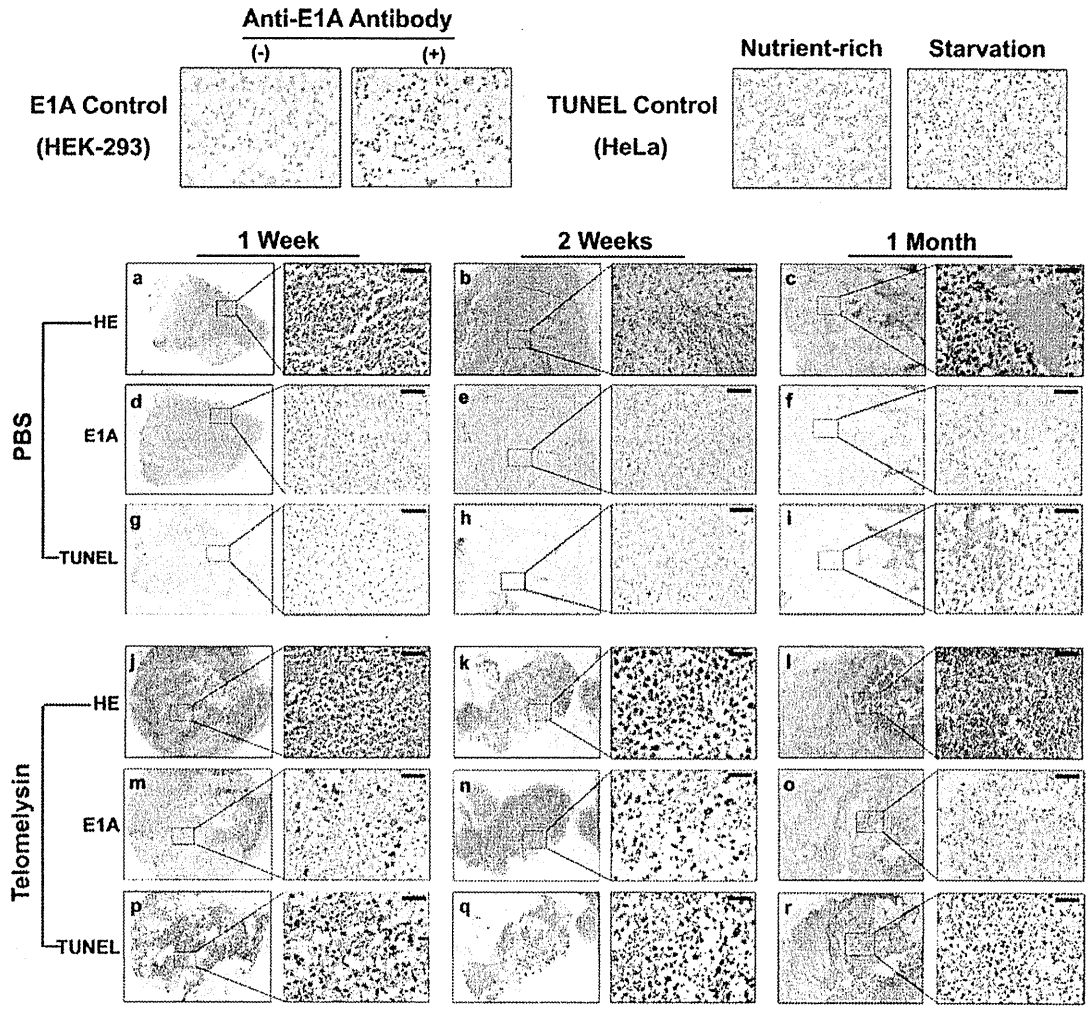

Fig. 7 Viral growth, lateral spread and subsequent induction of apoptotic cell death in NOS10-xenografted tumors of *nu/nu* mice following Telomelysin infection. Paraffin-embedded tumor sections were generated 1, 2 weeks and 1 month after the final intratumoral administration of PBS or Telomelysin. Histological evaluation was performed by hematoxylin and eosin staining (*top panel for each group*). Viral replication and spread was determined by immunohistochemical staining using the anti-adenovirus type 5 E1A antibody (*middle panel for each group*), and apoptotic cells were detected using a TUNEL assay (*bottom panel of each group*). Original magnification: ×20 for the left column and ×200 for the right column (magnified view of the boxed region). The *scale bar* represents 50 μm

time-dependent GFP expression and high viral infection rate, respectively, in these osteosarcoma cell lines, but not in normal cell lines NHDF and hMSC (Fig. 3a and b). These results demonstrated a positive strong association between the viral replication efficiency and the hTERT expression level, i.e., high-level hTERT activity led to high viral replication. Thus, we concluded that an adenovirus-based therapy using Telomelysin, in which the hTERT promoter directly controls adenoviral E1A and E1B gene transcription, may provide favorable anti-tumor efficacy against human osteosarcoma. As expected, Telomelysin was highly cytotoxic, in a dose-dependent manner, for osteosarcoma cell lines (Fig. 4). Telomelysin infection alone, at a low MOI of 0.1 or 1, was sufficient to induce significant tumor cell death of osteosarcoma cell lines, whereas no cytotoxicity was observed in NHDF and hMSC cell lines infected with Telomelysin (Fig. 4).

The precise molecular mechanism by which Telomelysin triggers cell death in human cancer remains unknown. Previous studies have noted that Telomelysin infection does not induce either apoptosis or any alteration of the cell cycle distribution in human lung cancer cells (Watanabe et al. 2006; Hioki et al. 2008). On the other hand, Telomelysin and Telomelysin-RGD have been reported to cause autophagic cell death in malignant glioma cells (Yokoyama et al. 2008). In the current study, we showed dose-dependent, Telomelysin-induced apoptosis in human osteosarcoma cell lines, which was indicated by the

appearance of activated caspase 3 and cleaved PARP (Fig. 5a). However, no increase in the ratio of LC3-II/I, a major marker for autophagy, was found in osteosarcoma cell lines treated with Telomelysin (Fig. 5b).

Previous studies have noted a low degree of viral replication in the Telomelysin-infected normal human lung fibroblast cell line, NHLF, despite the lack of an apparent cytopathic effect (Kawashima et al. 2004; Hashimoto et al. 2008; Taki et al. 2005). In this study, the normal human NHDF cell line and hMSCs also showed a low level of adenovirus replication following Telomelysin infection (Fig. 2, 3). It remains unclear why this low-level viral replication would occur in the hTERT-negative normal cell lines after Telomelysin infection, although its E1 gene expression is under the control of the hTERT promoter instead of the endogenous E1 promoter. However, a previous report has showed that even if the endogenous E1A promoter, including the transcription start site, was deleted, the adenovirus can still induce detectable E1A protein expression in normal human fibroblasts. This study proposed that the inverted terminal repeats (ITRs) located in the upstream sequence of the E1A promoter may result in leaky virus expression (Zheng et al. 2005). The adenovirus ITRs region contains cryptic transcription start sites that are essential for the initiation of viral DNA replication and for the packaging of viral particles (Osborne and Berk 1983; Hatfield and Hearing 1991). Therefore, the ITRs region must remain intact in all adenoviral vectors. Because Telomelysin is a recombinant adenoviral vector, its structure must also include the adenovirus ITRs region. It is therefore possible that low-level leaky Telomelysin replication might also occur in the normal cell lines. Nevertheless, in spite of this low level of viral replication, neither a cytotoxic effect nor apoptosis such as was seen in osteosarcoma cell lines, was observed in the normal NHDF cell lines or hMSC cell lines treated with Telomelysin (Figs. 4 and 5).

During adenovirus infection, the E1A protein binds to pRB of the host cell, thereby freeing E2F-1 to activate transcription and promote virus entry into the S-phase (Chiocca 2002). Viral replication can also elicit E2F-1-induced p53-dependent cell cycle arrest or apoptosis (Phillips et al. 1997; Chiocca 2002), and the E1B protein blocks p53 activity, thereby allowing continuous adenoviral replication (Yew and Berk 1992). In contrast, since p53 is frequently inactivated in osteosarcoma, Telomelysin could consistently replicate in these cells and induce intense cellular stress, ultimately causing apoptosis via a p53-independent pathway (Lavoie et al. 1998). However, in the current study, apoptosis was not observed in normal NHDF fibroblasts following Telomelysin infection, in spite of the presence of detectable expression of E1 mRNA and E1A protein. This lack of apoptosis induction in NHDF cell lines may be due to the possibility that the leaky E1 gene expression level may be too low to produce sufficient viral progeny release, cellular stress or DNA damage in the late stage. Further studies are warranted to clarify the precise mechanism by which Telomelysin induces tumor cell death, and whether the mechanism is cell type-dependent.

Our NOS10 in vivo xenograft model experiment also demonstrated the excellent oncolytic effect of Telomelysin. Intratumoral administration of Telomelysin induced significant suppression of the growth of xenografted NOS10 tumors over a long period of time (Fig. 6a and b). A high level of tumor-restricted E1 mRNA expression was detected in Telomelysin-treated tumors in the first 2 weeks after infection, and this expression was therefore maintained at a lower level for at least 1 month (Fig. 6c). Immunohistochemical staining confirmed a time-dependent increase in E1A protein expression over the first 2 weeks following the Telomelysin treatment of tumors (Fig. 7). However, the E1A protein was barely detected 1 month after infection, because almost all of the tumor cells had been eradicated by Telomelysin infection at this time point (Fig. 7). In line with the level of E1A protein expression, a time-dependent pronounced apoptotic cell death was also observed in the Telomelysin-treated tumor specimens. Based on these data, we therefore consider Telomelysin to be an effective anti-tumor adenoviral agent for the treatment of human osteosarcoma.

In conclusion, our data suggest that the telomerase-specific replication-selective adenovirus Telomelysin can effectively inhibit the cell growth of hTERT-positive human osteosarcoma cell lines both in vitro and in vivo. Since lung metastasis is the main cause of death for osteosarcoma patients, additional studies are therefore required to determine the effects of this novel tumor-targeted adenoviral agent in a model of lung metastatic osteosarcoma.

Acknowledgments We thank Keiko Tanaka and Yoshiaki Tanaka (Division of Orthopedic Surgery, Niigata University Graduate School of Medical and Dental Sciences) for their helpful assistance with the quantitative real-time RT-PCR and Western blotting assays.

References

Alemany M, Curiel DT (2000) The development of conditionally replicative adenovirus for cancer therapy. Clin Cancer Res 6:3395–3399

Bischoff JR, Kirn DH, Williams A, Heise C, Horn S, Muna M, Ng L, Nye JA, Sampson-Johannes A, Fattaey A, McCormick F (1996) An adenovirus mutant that replicates selectively in p53-deficient human tumor cells. Science 274:373–376

Chiocca EA (2002) Oncolytic viruses. Nat Rev Cancer 2:938–950

Dorfman HD, Czerniak B (1998) Osteosarcoma. In: Dorfman HD, Czerniak B (eds) Bone tumors, 1st edn. Mosby, St. Louis, pp 128–129

Fernandes-Alnemri T, Litwack G, Alnemri ES (1994) CPP32, a novel human apoptotic protein with homology to *Caenorhabditis elegans* cell death protein Ced-3 and mammalian interleukin-1 beta-converting enzyme. J Biol Chem 269:30761–30764

Fueyo J, Gomez-Manzano C, Alemany R, Lee PS, McDonnell TJ, Mitlianga P, Shi YX, Levin VA, Yung WK, Kyritsis AP (2000) A mutant oncolytic adenovirus targeting the RB pathway produces anti-glioma effect in vivo. Oncogene 19:2–12

Fujiwara T, Kagawa S, Kishimoto H, Endo Y, Hioki M, Ikeda Y, Sakai R, Urata Y, Tanaka N, Fujiwara T (2006) Enhanced antitumor efficacy of telomerase-selective oncolytic adenoviral agent OBP-401 with docetaxel: preclinical evaluation of chemovirotherapy. Int J Cancer 119:432–440

Fujiwara T, Tanaka N, Nemunaitis JJ, Senzer NN, Tong A, Ichimaru D, Shelby SM, Hashimoto Y, Kawamura H, Urata Y (2008) Phase I trial of intratumoral administration of OBP-301, a novel telomerase-specific oncolytic virus in patients with advanced solid cancer: evaluation of biodistribution and immune response. J Clin Oncol 26:171s

Goorin AM, Schwartzentruber DJ, Grier HE, Link MP (2003) Presurgical chemotherapy compared with immediate surgery and adjuvant chemotherapy for nonmetastatic osteosarcoma: Pediatric Oncology Group Study POG-8651. J Clin Oncol 21:1574–1580

Gu W, Ogose A, Kawashima H, Ito M, Ito T, Matsuba A, Kitahara H, Hotta T, Tokunaga K, Hatano H, Morita T, Urakawa S, Yoshizawa T, Kawashima H, Kuwano R, Endo N (2004) High-level expression of the coxsackievirus and adenovirus receptor messenger RNA in osteosarcoma, Ewing's sarcoma, and benign neurogenic tumors among musculoskeletal tumors. Clin Cancer Res 10:3831–3838

Harada JN, Berk AJ (1999) p53-independent and -dependent requirements for E1B–55 k in adenovirus type 5 replication. J. Virol 73:5333–5344

Hashimoto Y, Watanabe Y, Shirakiya Y, Uno F, Kagawa S, Kawamura H, Nagai K, Tanaka N, Kumon H, Urata Y, Fujiwara T (2008) Establishment of biological and pharmacokinetic assays of telomerase-specific replication-selective adenovirus. Cancer Sci 99:385–390

Hatfield L, Hearing P (1991) Redundant elements in the adenovirus type 5 inverted terminal repeat promote bidirectional transcription in vitro and are important for virus growth in vivo. Virology 184:265–276

Heise C, Hermiston T, Johnson L, Brooks G, Sampson-Johannes A, Williams A, Hawkins L, Kirn D (2000) An adenovirus E1A mutant that demonstrates potent and selective systemic anti-tumoral efficacy. Nat Med 6:1134–1139

Hioki M, Kagawa S, Fujiwara T, Sakai R, Kojima T, Watanabe Y, Hashimoto Y, Uno F, Tanaka N, Fujiwara T (2008) Combination of oncolytic adenovirotherapy and Bax gene therapy in human cancer xenografted models. Potential merits and hurdles for combination therapy. Int J Cancer 122:2628–2633

Horner MJ, Ries LAG, Krapcho M, Neyman N, Aminou R, Howlader N, Altekruse SF, Feuer EJ, Huang L, Mariotto A, Miller BA, Lewis DR, Eisner MP, Stinchcomb DG, Edwards BK (2009) SEER cancer statistics review, 1975–2006, National Cancer Institute. Bethesda. http://seer.cancer.gov/csr/1975_2006/, based on November 2008 SEER data submission, posted to the SEER web site, 2009. Accessed 10 March 2010

Hotta T, Motoyama T, Watanabe H (1992) Three human osteosarcoma cell lines exhibiting different phenotypic expressions. Acta Pathol Jpn 42:595–603

Irving J, Wang Z, Powell S, O'Sullivan C, Mok M, Murphy B, Cardoza L, Lebkowski JS, Majumdar AS (2004) Conditionally replicative adenovirus driven by the human telomerase promoter provides broad-spectrum antitumor activity without liver toxicity. Cancer Gene Ther 11:174–185

Kabeya Y, Mizushima N, Yamamoto A, Oshitani-Okamoto S, Ohsumi Y, Yoshimori T (2004) LC3, GABARAP and GATE16 localize to autophagosomal membrane depending on form-II formation. J Cell Sci 117:2805–2812

Kawashima T, Kagawa S, Kobayashi N, Shirakiya Y, Umeoka T, Teraishi F, Taki M, Kyo S, Tanaka N, Fujiwara T (2004) Telomerase-specific replication-selective virotherapy for human cancer. Clin Cancer Res 10:285–292

Kim NW, Piatyszek MA, Prowse KR, Harley CB, West MD, Ho PL, Coviello GM, Wright WE, Weinrich SL, Shay JW (1994) Specific association of human telomerase activity with immortal cells and cancer. Science 266:2011–2015

Kirn D (2001) Clinical research results with dl1520 (Onyx-015), a replication-selective adenovirus for the treatment of cancer: what have we learned? Gene Ther 8:89–98

Kirn D, Martuza RL, Zwiebel J (2001) Replication-selective virotherapy for cancer: biological principles, risk management and future directions. Nat Med 7:781–787

Kishimoto H, Kojima T, Watanabe Y, Kagawa S, Fujiwara T, Uno F, Teraishi F, Kyo S, Mizuguchi H, Hashimoto Y, Urata Y, Tanaka N, Fujiwara T (2006) In vivo imaging of lymph node metastasis with telomerase-specific replication-selective adenovirus. Nat Med 12:1213–1219

Lavoie JN, Nguyen M, Marcellus RC, Branton PE, Shore GC (1998) E4orf4, a novel adenovirus death factor that induces p53-independent apoptosis by a pathway that is not inhibited by zVAD-fmk. J Cell Biol 140:637–645

Leppard KN, Shenk T (1989) The adenovirus E1B 55 kd protein influences mRNA transport via an intranuclear effect on RNA metabolism. EMBO J 8:2329–2336

Lewis IJ, Nooij MA, Whelan J, Sydes MR, Grimer R, Hogendoorn PC, Memon MA, Weeden S, Uscinska BM, van Glabbeke M, Kirkpatrick A, Hauben EI, Craft AW, Taminiau AH MRC, MRC BO06 and EORTC 80931 collaborators; European Osteosarcoma Intergroup (2007) Improvement in histologic response but not survival in osteosarcoma patients treated with intensified chemotherapy: a randomized phase III trial of the European Osteosarcoma intergroup. J Natl Cancer Inst 99:112–128

Li G, Ogose A, Kawashima H, Umezu H, Hotta T, Tohyama T, Ariizumi T, Endo N (2009) Cytogenetic and real-time quantitative reverse-transcriptase polymerase chain reaction analyses in pleomorphic rhabdomyosarcoma. Cancer Genet Cytogent 192:1–9

Meyerson M, Counter CM, Eaton EN, Ellisen LW, Steiner P, Caddle SD, Ziaugra L, Beijersbergen RL, Davidoff MJ, Liu Q, Bacchetti S, Haber DA, Weinberg RA (1997) hEST2, the putative human telomerase catalytic subunit gene, is up-regulated in tumor cells and during immortalization. Cell 90:785–795

Oliver FJ, de la Rubia G, Rolli V, Ruiz-Ruiz MC, de Murcia G, Murcia JM (1998) Importance of poly(ADP-ribose) polymerase and its cleavage in apoptosis. Lesson from an uncleavable mutant. J Biol Chem 273:33533–33539

Osborne TF, Berk AJ (1983) Far upstream initiation sites for adenovirus early region 1A transcription are utilized after the onset of viral DNA replication. J Virol 45:594–599

Phillips AC, Bates S, Ryan KM, Helin K, Vousden KH (1997) Induction of DNA synthesis and apoptosis are separable functions of E2F–1. Genes Dev 11:1853–1863

Rodriguez R, Schuur ER, Lim HY, Henderson GA, Simons JW, Henderson DR (1997) Prostate attenuated replication competent adenovirus (ARCA) CN706: a selective cytotoxic for prostate-specific antigen-positive prostate cancer cells. Cancer Res 57:2559–2563